A Novel Approach to Sustainable Bio-Lubricant and Biodiesel Production Using Yeast-Microalgae Co-Cultivation in Hydrolyzed PPMS

Abstract

Bioprocess engineering and waste valorization offer a promising pathway for sustainable bio-lubricant, biodiesel, and carotenoid production. This study explores the potential of pulp and paper mill sludge (PPMS) as a carbon-rich resource for microbial lipid and carotenoid synthesis through the co-cultivation of the oleaginous yeast *Rhodosporidium babjevae* and the microalga *Arthrospira platensis*. To maximize sugar release from PPMS, a two-step hydrolysis process was carefully optimized. Acid hydrolysis, fine-tuned using Central Composite Design (CCD), was carried out with a sulfuric-nitric acid mixture (6.794% w/w) at 139°C for 16.06 minutes, yielding a reducing sugar index of 1.051. This was followed by enzymatic hydrolysis (2% w/w enzyme, 50°C, 150 rpm, 72 hours) to further enhance sugar availability. The co-cultivation process was optimized using Box-Behnken Design (BBD), leading to a lipid yield of 6.683 g/L, a carotenoid yield of 25.099 mg/L, a biomass concentration of 8.659 g/L, and an impressive COD removal efficiency of 86.762% under the best conditions (light intensity: 3.8 Klux, airflow: 1.4 L/min, duration: 5.7 days, microalgae-to-yeast ratio: 2.6). The extracted lipids showed a favorable fatty acid profile suitable for bio-lubricant and biodiesel applications. Beyond bioproduct synthesis, this process also contributed significantly to wastewater treatment and sludge remediation, demonstrating its potential for both environmental and industrial sustainability. This study highlights the feasibility of transforming industrial waste into valuable bioproducts while promoting cleaner production strategies.

Keywords: Bio-lubricant, Biodiesel, Yeast-Microalgae Co-Cultivation, Hydrolyzed PPMS, Carotenoid extraction, COD removal.

1. Introduction

The global energy crisis, which is primarily driven by dependency on fossil fuels and growing greenhouse gas emissions (GHGs), emphasizes the vital need for sustainable alternatives like biodiesel and bio-lubricants. Fossil fuels account for over 75% of global GHG emissions, with transportation and industry being the largest sources (IEA, 2019). According to Ananthi et al. (2021), biodiesel derived from fatty acid methyl esters (FAMEs) can reduce net carbon emissions by 50-80% when compared to standard petro-diesel. Similarly, bio-lubricants derived from renewable oils are more biodegradable and safer than mineral oil alternatives (Sharma et al. 2016). Despite these benefits, traditional biodiesel production is hampered by problems such as the scalability of monoculture-based microbial systems, rivalry with food crops, and high pretreatment costs for lignocellulosic biomass (Patel et al., 2020). Third-generation feedstocks, particularly oleaginous microorganisms such as yeasts and microalgae, have showed tremendous promise due to their quick growth rates, high lipid synthesis, and capacity to flourish in industrial waste streams (Khan et al., 2018).

Bio-lubricants derived from lignocellulosic waste represent a possible renewable answer to the need for industrial lubricants, lowering dependency on existing oil-based alternatives. However, the long-term economic sustainability of generating bio-lubricants from plants remains uncertain due to the significant expenses involved. The utilization of oleaginous microorganisms, such as yeasts, microalgae, and bacteria, offers a novel, cost-effective, and ecologically friendly alternative to bio-lubricant manufacturing. Microbial oils, which have fatty acid profiles comparable to plant oils, can be used as efficient alternatives. Furthermore, employing microbial sources, particularly yeasts that can thrive in industrial effluents, can lower production costs while also addressing environmental issues by reducing industrial wastewater pollution (Pradhan et al., 2024; Papadaki et al., 2018). Yeasts and microalgae excel in converting CO_2 into biofuels such as methane, biohydrogen, and oils, making them unique among oleaginous microbes. Microalgae may thrive in fermentation tanks or even wastewater systems, but yeasts can create vast amounts of lipids with characteristics similar to plant oils. Furthermore, yeasts grow quickly and are inexpensive to produce (Nguyen et al., 2024; Ma et al., 2021).

Co-cultivation of yeast and microalgae in industrial effluents has emerged as a cost-effective and ecologically friendly technique for producing bio-lubricants. Mixed microbial cultures are commonly employed to remediate industrial waste, generate biomass, and produce bioactive chemicals. Co-cultivation has been shown in studies to considerably improve microbial system efficiency and total production. This approach helps to reduce global greenhouse gas emissions while also protecting aquatic habitats and developing renewable energy resources (Cheirsilp et al., 2011).

One promising candidate for bio-lubricant production is *Arthrospira platensis* (Spirulina), a versatile cyanobacterium that has gained attention for its potential in sustainable biofuel generation. Although *A. platensis* is well-known for its high protein content (60–70% of dry weight) and nutritional value, it can also adapt to various cultivation conditions, including nitrogen and phosphorus deprivation, which enhances lipid accumulation by up to 20% under optimal nutrient stress (Baunillo et al., 2012). For example, under nitrogen and phosphate-limited conditions, *A. platensis* can increase its lipid production by 20%, with FAME profiles dominated by C16:0 and C18:2 fatty acids, which align with biodiesel requirements. Furthermore, mixotrophic cultivation, using seawater and brewery wastewater (BWW), not only enhances lipid production but also increases the proportions of C16:0 and C18:1 FAMEs, important for fuel stability (Russo et al., 2024). Hydrothermal liquefaction of *A. platensis* biomass yields bio-oils with up to 13.8 weight percent, though further refinement is needed to reduce the polar compound content. Additionally, the lipid-free biomass can be used as feed for marine rotifers or for bioremediation purposes, such as efficiently removing dye from textile effluents (75.7% efficiency).

Pulp and paper mill sludge (PPMS), a lignocellulosic waste produced at a rate of 40–50 kg per ton of paper, represents an untapped resource, with an annual global output exceeding 50 million metric tons (Khoo et al., 2019). PPMS is rich in cellulose, hemicellulose, and lignin, but its microbial conversion is hindered by inhibitors such as phenolics, ligno-carbohydrate complexes,

and high ash content. Acid hydrolysis, particularly with sulfuric acid (2% v/v), releases fermentable sugars like glucose and xylose, improving solid load efficiency and reducing CO_2 emissions by 25% compared to untreated biomass (Sharma et al., 2016). These hydrolysates can serve as low-cost substrates for microbial lipid production, aligning with the principles of a circular economy by converting waste into energy (Mathimani & Pugazhendhi, 2019).

Oleaginous yeast species, such as *Yarrowia lipolytica*, *Rhodotorula glutinis*, and *Rhodosporidium toruloides*, can accumulate up to 70% of their dry weight as lipids under nitrogen-limited conditions, with fatty acid profiles rich in C16–C18 chains, ideal for biodiesel synthesis (Patel et al., 2020). For instance, *R. glutinis* achieves a cetane number of 71.58, surpassing petro-diesel standards (Cheirsilp et al., 2011), while *Cryptococcus curvatus* demonstrates lipid yields of 51.9% when grown on lignocellulosic hydrolysates (Chatterjee & Mohan, 2018). Microalgae like *Chlorella* and *Scenedesmus*, in combination with yeast, fix CO_2 through photosynthesis and contribute to carbon sequestration, producing lipids (10–40% of dry weight) and bioactive compounds (Goswami et al., 2021). However, monocultures face several challenges: microalgae exhibit poor lipid yields under autotrophic conditions, and high harvesting costs are a concern, while yeast requires expensive organic substrates (Yen et al., 2015).

Co-cultivation systems capitalize on mutualistic interactions to address these challenges. Microalgae supply oxygen and organic carbon to yeast, while yeast metabolizes complex substrates, releasing CO_2 and nutrients such as nitrogen and phosphorus for algal growth (Magdouli et al., 2016). Co-cultures of *Chlorella sorokiniana* and *R. glutinis* have demonstrated a 30% increase in lipid productivity compared to monocultures, along with phosphate removal from wastewater (Zhang et al., 2014). Furthermore, the acidic pH (<6) preferred by yeast inhibits bacterial growth, and microalgae-yeast flocs, which form self-settling aggregates, reduce centrifugation costs by 40% and minimize contamination risks (Liu et al., 2018).

A promising approach combines microbial co-cultivation with PPMS valorization, offering a dual-output biorefinery. Heterogeneous catalysts, such as magnesium silicates, can transesterify lipids extracted by ultrasound, doubling the effectiveness of traditional solvent methods, achieving FAME conversions exceeding 90% (Mohiddin et al., 2021). The economic feasibility of co-producing biodiesel and high-value co-products from systems like *Pichia guilliermondii* is further enhanced by the functionalization of residual lipids, rich in unsaturated fatty acids like oleic (C18:1) and linoleic acid (C18:2), into bio-lubricants through epoxidation or esterification (Lian et al., 2018).

Despite these advancements, challenges persist. PPMS composition varies seasonally, requiring adaptive pretreatment protocols, and optimizing pH, temperature, and nutrient ratios for co-cultivation remains complex (Sánchez-Solís et al., 2024). Fed-batch fermentation, which alleviates carbon source inhibition, can improve lipid yields by 35–80%. Additionally, genetic engineering of yeast and microalgae strains can enhance lipid synthesis pathways. For instance, synthetic biology tools have enabled *Y. lipolytica* to overexpress acyl-CoA diacylglycerol acyltransferase (DGA1), boosting lipid accumulation by 40% (Patel et al., 2020). Omics technologies have also identified stress-resistant microalgae strains capable of utilizing high inorganic carbon

concentrations, although outdoor cultivation of genetically modified organisms requires rigorous risk assessments (Lian et al., 2018).

In conclusion, the co-cultivation of yeast and microalgae in hydrolyzed PPMS presents a groundbreaking strategy for the sustainable production of bio-lubricants and biodiesel. This approach not only addresses feedstock availability, process efficiency, and environmental impact but also aligns with the United Nations Sustainable Development Goals (UN SDGs) and the principles of the circular bioeconomy. Future research should focus on techno-economic evaluations, AI-driven bioreactor optimization, and policy frameworks to scale these innovations and contribute to achieving net-zero emissions (Ananthi et al., 2021).

By utilizing yeast-microalgae co-cultivation in hydrolyzed PPMS, we aim to establish a sustainable and innovative method for simultaneous production of bio-lubricants and biodiesel. This strategy focuses on maximizing the conversion of lignocellulosic biomass into valuable biofuels and lubricants, while addressing environmental challenges associated with industrial waste disposal. Through a synergistic combination of *Arthrospira platensis* and *Rhodosporidium babjevae*, we seek to optimize substrate utilization, improve fatty acid profiles, and enhance lipid accumulation. Acid and enzymatic hydrolysis will be employed to achieve optimal breakdown of PPMS into fermentable sugars, facilitating enhanced microbial growth and lipid biosynthesis. By utilizing experimental design methodologies such as CCD and BBD, we will identify the ideal conditions for hydrolysis and cultivation, ensuring the highest yields and quality of bio-based products.

2. Materials and Methods

2.1. Preparation and Hydrolysis of PPMS

In this study, PPMS from the wood and paper industries in Mazandaran was sourced specifically for printing and newspaper applications, without prior biological treatment. The yeast *Rhodosporidium babjevae* and microalga *Arthrospira platensis* were obtained from the National Center for Genetic and Biological Resources of Iran. Cellulase, an enzyme derived from *Aspergillus niger*, was used to break down the PPMS. FTIR analysis indicated that hydrolysis was necessary to improve sugar bioavailability for microbial utilization. To achieve this, both acidic and enzymatic hydrolysis processes were applied.

The optimal conditions for acidic hydrolysis were found to be 139°C for 16.06 minutes, with sulfuric and nitric acids at concentrations of 3.181% and 3.608%, respectively. The key parameters for acidic hydrolysis comprised temperature (100-140°C), duration (10-60 minutes), acid concentration (1-7% w/w), and the ratio of nitric to sulfuric acid, represented by β. The pH was adjusted to 5 using sodium citrate buffer. Following that, enzymatic hydrolysis was performed at 50°C for 72 hours using a 2% enzyme concentration.

Enzymatic hydrolysis was carried out in a laboratory incubator shaker set to 150 rpm, with the sugar content closely measured throughout using the DNS technique. The sugar content quadrupled after the acidic hydrolysis stage, and enzymatic hydrolysis boosted it to four times its original level (Shi et al., 2020; Sun et al., 2019). These experimental settings were chosen after

preliminary testing with different enzyme concentrations (1%, 2%, and 3% w/w), shaker speeds (150 rpm), hydrolysis periods (3, 1, and 5 days), and a constant temperature of 50°C. The objective was to have the maximum concentration of reducing sugars. Furthermore, 1% (w/w) of polyethylene glycol was added to all experimental setups to facilitate the reaction.

The DNS method was employed to measure the concentration of reducing sugars by reacting them with 3,5-dinitrosalicylic acid, forming a red-orange complex. The intensity of the color, which is directly proportional to the sugar concentration, was measured at a wavelength of 540 nm. To prepare the DNS reagent, potassium sodium tartrate and 3,5-dinitrosalicylic acid were dissolved in NaOH, and the solution was diluted accordingly. In the assay, 3 mL of the sample was mixed with 1 mL of the DNS reagent and heated in a boiling water bath for 5 minutes. After cooling to room temperature, the absorbance was measured. It is important to note that precise temperature control was essential, as the absorbance is highly temperature-dependent.

Upon completing the hydrolysis process, the resulting wastewater was filtered using a Buchner funnel and 0.2-micron filter paper to eliminate any coarse particles. The resulting hydrolyzed wastewater, referred to as HPPMS (Hydrolyzed PPMS), was then utilized as the co-culture medium for yeast and microalgae in the subsequent stages of the study.

2.2. Pure Cultivation of Microorganisms

2.2.1. Yeast Cultivation

The yeast strain was originally cultivated on solid medium before being moved to a liquid YM media for continued growth. The YM medium for one liter contained glucose (10 g), peptone (5 g), yeast extract (3 g), and malt extract (3 g) (Tahmasebi et al., 2024). Cultivation was conducted in 1-liter graded cylinders with moderate light intensity, ambient temperature, and a 16-hour light/8-hour dark cycle. To ensure proper mixing, an aeration system consisting of pumps and air stones was used. The yeast culture was allowed to develop for three days under these circumstances. After the first development phase in YM medium, a progressive adaptation procedure was started to acclimate the yeast to the HPPMS media. In this step, 200 mL of yeast culture was transferred to a fresh medium containing 90% YM and 10% HPPMS. This method was repeated in each consecutive batch, with a 20% rise in HPPMS, until the culture had fully acclimated to the HPPMS medium, at which point the medium was 100% HPPMS.

When the yeast culture had finished growing in HPPMS, it was collected and prepared for storage. The yeast culture from the 1-liter graduated cylinder was transferred to 50-mL Falcon tubes and centrifuged at 10,000 rpm for 15 minutes to separate the cells from the media. The supernatant was carefully discarded, with a fraction saved for COD testing. The yeast cells that accumulated at the bottom of the Falcon tubes were transferred to petri plates and dried in an oven at 55°C for 24 hours. After drying, the HPPMS-adapted yeast was scraped from the petri dishes with a spatula, powdered, and stored in sealed glass containers at room temperature for future experimental use.

2.2.2. Microalgae Cultivation

The microalga strain was initially cultivated on solid medium and then transferred to liquid Zarrouk Medium for further growth. The composition of the liquid Zarrouk Medium for 1 liter included $NaHCO_3$ (13.61 g), K_2HPO_4 (0.5 g), Na_2CO_3 (4.03 g), $NaNO_3$ (2.5 g), K_2SO_4 (1 g), NaCl

(1 g), $MgSO_4 \cdot 7H_2O$ (0.2 g), $CaCl_2 \cdot 2H_2O$ (0.04 g), $FeSO_4 \cdot 7H_2O$ (0.01 g), EDTA (titriplex III, 0.08 g), and 5 mL of a micronutrient solution (Aiba & Ogawa, 1977). The micronutrient solution was prepared by dissolving $ZnSO_4 \cdot 7H_2O$ (1 mL), $MnSO_4 \cdot 4H_2O$ (2 mL), H_3BO_3 (5 mL), $Co(NO_3)_2 \cdot 6H_2O$ (5 mL), $Na_2MoO_4 \cdot 2H_2O$ (5 mL), $CuSO_4 \cdot 5H_2O$ (1 mL), EDTA (0.4 g), and $FeSO_4 \cdot 7H_2O$ (0.7 g) in 1 liter of distilled water.

The cultivation of the microalga took place in 1-liter graduated cylinders under moderate light intensity, ambient temperature, and a 16-hour light/8-hour dark cycle over a 14-day growth period. Aeration and mixing were achieved using pumps and air stones to maintain optimal conditions for the microalga.

The microalga was adapted to the HPPMS medium following the same technique as the yeast. Following the adaption phase, the microalgae were separated from the medium. This technique involves centrifugation to remove the liquid, followed by 24 hours of drying at 55°C. The dried microalgae were crushed into a fine powder and kept in sealed glass containers at room temperature for later use in experiments.

2.3. Co-Cultivation of Yeast and Microalgae

After the yeast and microalgae were prepared as powders and adapted to the HPPMS medium, they were co-cultivated in a single medium to assess the enhanced lipid production and COD removal efficiency compared to their individual monocultures.

Given the complexity of co-cultivation, a set of critical parameters was identified to optimize the process. These parameters were chosen based on their potential impact on the overall performance of the co-culture. An experimental design was developed to explore the influence of these factors and determine the ideal conditions for achieving the highest biomass concentration, lipid production (expressed in grams per liter), and COD removal efficiency.

The following key parameters were selected for the co-cultivation process, along with the ranges for each, which guided the experimental setup using the BBD method:

1. **Yeast to Microalgae Ratio**:
    - 1:1, 2:1, 3:1
2. **Light Intensity (Klux)**:
    - 2, 4, 6
3. **Air Flow Rate for Mixing (L/min)**:
    - 0.5, 1, 1.5
4. **Cultivation Duration (Days)**:
    - 3, 5, 7

The co-cultivation tests were carried out in 1-liter graduated cylinders that were sealed with foil and well cleaned to avoid contamination. For each trial, yeast and microalgae powders were weighed and mixed into the growth medium at the prescribed ratio. Pumps and air stones were used to mix the media, ensuring optimum aeration and microbe dispersion. The air flow rate, which influences mixing efficiency, was precisely regulated with a flow meter and varied by altering the pump speed.

To regulate light intensity, a fluorescent light system was employed. The intensity was adjusted by changing the distance between the cylinders and the light source, with the exact light intensity for each condition measured using a lux meter.

Cultivation duration was selected in accordance with the experimental design, allowing for variation in the length of the cultivation period across different trials.

At the end of each experimental run, the biomass concentration, lipid production, carotenoid yields, and COD removal efficiency were measured to evaluate the effectiveness of each set of conditions. This comprehensive assessment helped to identify the optimal co-cultivation parameters that maximize both lipid production and COD removal efficiency.

2.4. Carotenoid Extraction

To extract carotenoids from microorganisms grown under varying conditions (monoculture of microalgae, monoculture of yeast, and mixed culture), the following extraction procedure was employed after the completion of the growth period in each sample:

First, a portion of the grown culture was transferred into a Falcon tube and centrifuged at 10,000 rpm for 15 minutes to separate the culture medium from the cells. The carotenoid extraction was carried out using a dry extraction method, similar to the drying process for yeast.

Following the drying process, around 0.1 grams of dried microorganisms were transferred to a Falcon tube. To start the extraction, 2 mL of preheated dimethyl sulfoxide (DMSO) at 40°C was added. The tube was vortexed for 1 minute before being kept at room temperature for 10 minutes. Following that, 5 mL of acetone was added to the tube, which was vortexed again before being sonicated at 50% power for 10 minutes in an ultrasonic bath.

Subsequently, the Falcon tube was centrifuged at 4,500 rpm for 10 minutes. The supernatant was discarded, and the acetone addition and vertexing steps were repeated until the material at the bottom of the tube turned a grayish color, indicating that the carotenoids had been sufficiently extracted. This step was carried out twice for each sample.

Finally, the residue in the Falcon tube was filtered through a 22-micron membrane filter, and the absorbance of the filtered sample was measured at 480 nm using a spectrophotometer. The absorbance value was then used to calculate the total carotenoid content using the appropriate formula.

Total carotenoid content (mg/g microorganism) = $(A_{max} \times D \times V) / (E \times W)$

Where:

- A_{max} = maximum absorbance at 480 nm
- D = dilution factor of the sample
- V = volume of solvent used
- E = total carotenoid extinction coefficient (0.16)
- W = weight of dried microorganism

Using this method, the total carotenoid content was extracted and measured for all samples (Cheng & Yang, 2016; Michelon et al., 2012).

2.5. Lipid Extraction

The Bligh-Dyer technique (Bligh & Dyer, 1959) was used for lipid extraction, employing a Soxhlet extraction equipment and a methanol-chloroform solvent combination (2:1). Following the growing phase, the microorganism was centrifuged at 10,000 rpm for 15 minutes to separate the culture media. A portion of the medium was reserved for COD analysis. Unlike carotenoid extraction, lipid extraction was performed in a wet state, hence no drying was required. To increase extraction efficiency, the microbial biomass was treated with 5 mL of methanol and then ultrasonically treated. The treated biomass was then subjected to Soxhlet extraction with 190 mL methanol and 95 mL chloroform for 24 hours at 65°C. The microbial lipids were collected and purified using a rotary evaporator, removing the solvents under reduced pressure. Finally, the lipids were stored in glass containers at 25°C for further analysis.

2.6. Transesterification and Bio-lubricant Production

To improve the thermal value of the extracted lipid, an esterification process was carried out by mixing microbial oil with methanol in a 1:5 ratio, using potassium hydroxide (KOH) as a catalyst at 1% weight of the oil. This mixture was heated at 60°C for 1 hour, resulting in a two-phase solution after 24 hours. The glycerol phase was separated, and the methyl esters of FAMEs were stored. A second transesterification step followed to further refine the FAMEs, reacting them with neopentyl glycol (NPG) and sodium methoxide (1.5 wt.%) at 120°C for 90 minutes, removing methanol through distillation. To boost the bio-lubricant's properties, performance-enhancing additives—polymethyl methacrylate (PMMA, 1 wt.%), butylated hydroxytoluene (BHT, 0.1 wt.%), and titanium dioxide (TiO_2) nanoparticles (0.5 wt.%)—were incorporated to improve viscosity, antioxidant properties, and thermal stability. This process not only improves the quality of the bio-lubricant but also makes the process more efficient by recovering methanol and glycerol, reducing waste. This approach offers a more sustainable, eco-friendly method for producing bio-lubricants, relying on renewable resources instead of fossil-based alternatives (Moncada et al., 2016; Checa et al., 2020; Encinar et al., 2021).

2.7. Analytical Methods

This study explores the fatty acid profile and key physicochemical properties of a bio-lubricant produced from lignocellulosic waste. FAMEs were extracted using a modified Bligh and Dyer method and analyzed with an Agilent 7890A gas chromatograph (GC), equipped with a flame ionization detector (FID). The separation process utilized a DB-23 capillary column and helium as the carrier gas, flowing at 1.8 mL/min. To evaluate the bio-lubricant's performance, its physicochemical properties were measured according to ASTM standards, including kinematic viscosity (ASTM D445-17a), density (ASTM D4052-22), flash point (ASTM D92), pour point (ASTM D97-08), sulfated ash content (ASTM D874-23), and total acid number (ASTM D974-22). The environmental impact was assessed by measuring COD using the standard colorimetric method (5220D). The bio-lubricant's oxidation stability was determined with the Rancimat method (EN 14112), while its low-temperature operability was assessed using the cold filter plugging point (CFPP) method (ASTM D6371-17a). Finally, the iodine value, which indicates the degree of unsaturation in the bio-lubricant, was measured using the Wijs method (ASTM D1959-97). These

comprehensive analyses provide valuable insights into the bio-lubricant's potential for industrial applications, while also addressing its environmental performance.

3. Results and Discussion

3.1. Analysis of the Prepared PPMS Sample

The FTIR spectrum analysis of the prepared PPMS sample is presented below.

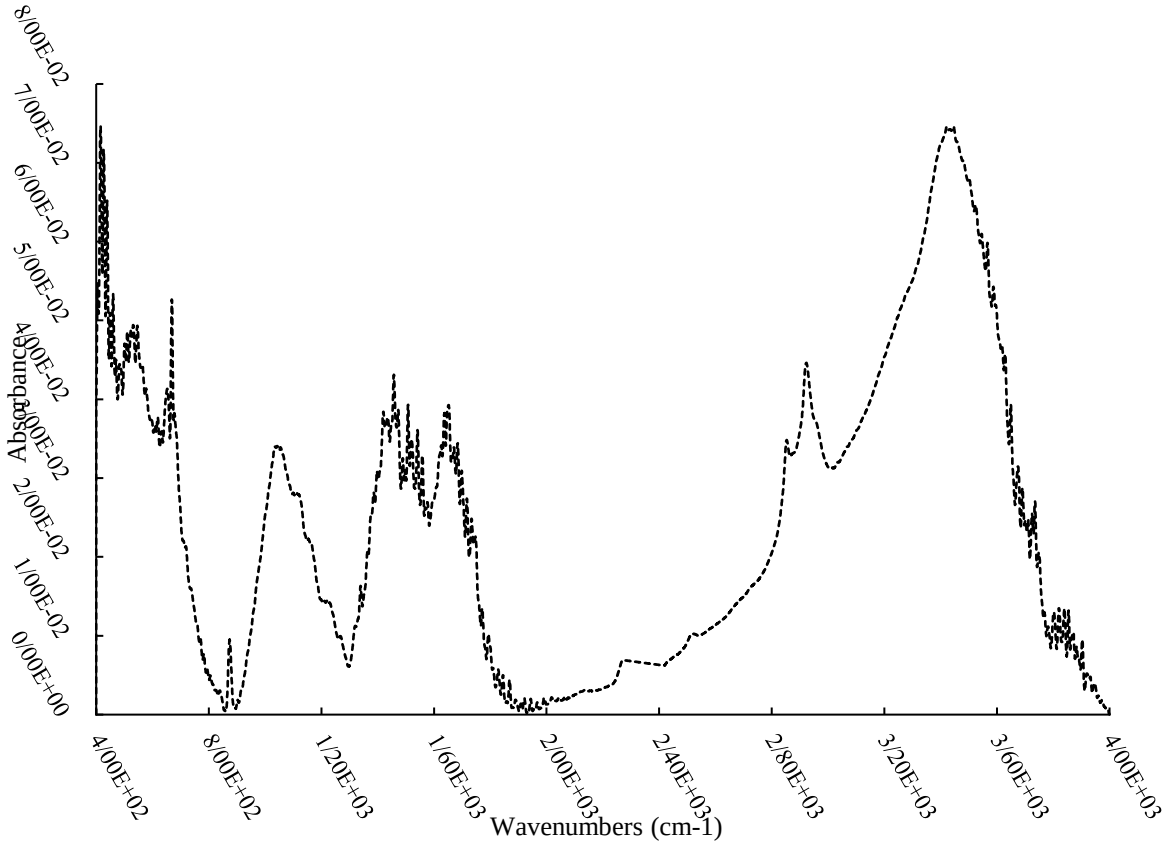

Figure 1: FTIR Spectrum of the PPMS Sample

FTIR spectroscopy was employed to analyze the chemical composition and structural properties of PPMS. The spectra revealed key functional groups, such as hydroxyl (-OH) stretches (3200–3600 cm^{-1}), which indicated a high content of cellulose and hemicellulose, as well as aliphatic (C-H) stretches (2800–3000 cm^{-1}), reflecting the integrity of the biomass. Carbonyl (C=O) bands (1650–1720 cm^{-1}) and aromatic (C=C) stretches (1515 cm^{-1}) pointed to the presence of lignin and hemicellulose. Notably, significant structural changes were observed following various pretreatment methods. Enzymatic hydrolysis led to increased absorption in the 1330–1420 cm^{-1} region, which is indicative of effective hemicellulose degradation. Additionally, nitric acid hydrolysis, particularly when combined with enzymatic treatment, enhanced lignin breakdown and improved polysaccharide accessibility. These results underscore the effectiveness of combining

acid and enzyme treatments to improve biomass fractionation, as reflected by the marked spectral changes, particularly in the lignin and hemicellulose regions (Jackson et al., 1997; Jiang et al., 2024; Ottah et al., 2022).

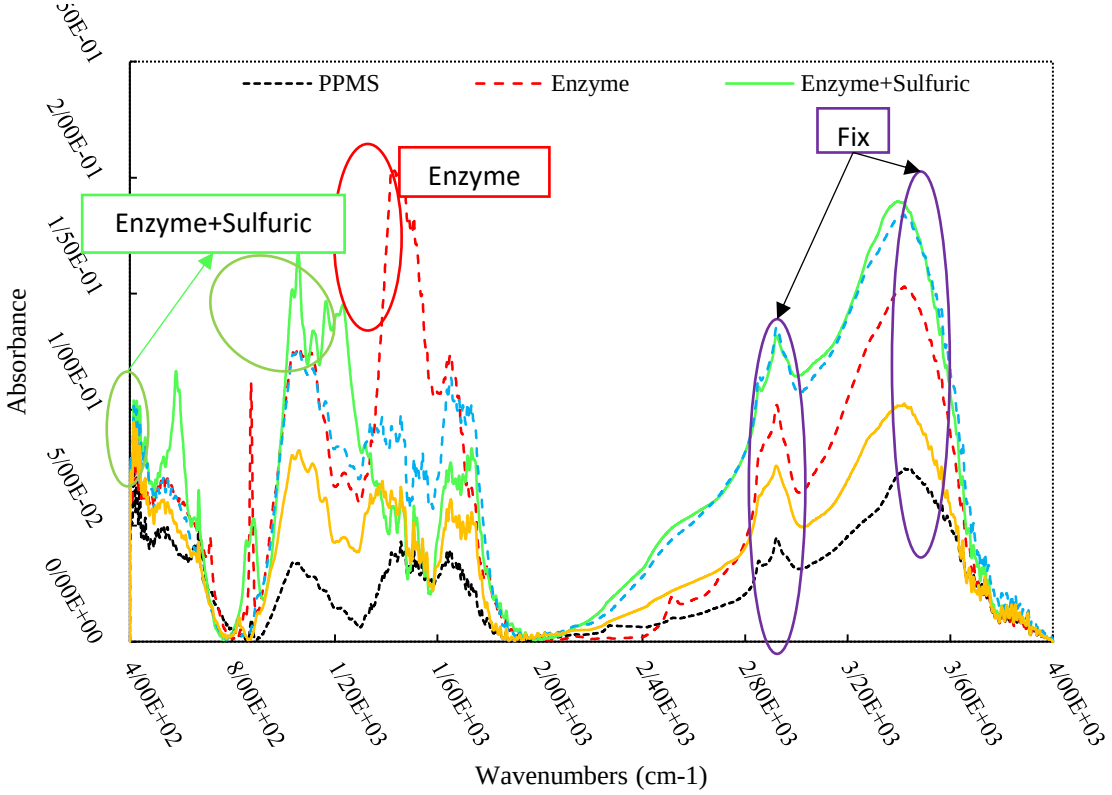

Figure 2: FTIR Spectra of the Samples

3.2. Optimization of the Acid Hydrolysis Process

In this part, the concentration of reducing sugars, measured as the response variable, was used as a critical performance indicator to optimise the acid hydrolysis process. The reducing sugar content was determined using the 3,5-dinitrosalicylic acid (DNS) test after enzymatic hydrolysis, which was carried out under controlled conditions: an enzyme concentration of 2% (w/w), a temperature of 50°C, a shaking speed of 150 rpm, and a reaction period of 72 hours. Notably, increasing the enzyme concentration or prolonging the hydrolysis period beyond these limits resulted in a decrease in DNS values, implying enzymatic inhibition or substrate depletion.

To establish a predictive framework for the acid hydrolysis process, a mathematical model was developed to estimate the reducing sugar index based on DNS measurements. This model facilitated the identification of optimal hydrolysis conditions, which were subsequently validated through experimental trials.

3.2.1 Optimized Conditions and Experimental Validation

The model-derived optimal conditions for acid hydrolysis were as follows:

- β Value: 0.063
- Acid Concentration: 6.794% (w/w)

- Temperature: 139.8°C
- Reaction Time: 16.06 minutes
- Predicted Reducing Sugar Index (Y): 1.051

To verify the reliability of these optimized conditions, acid hydrolysis experiments were conducted in triplicate, and the experimental results are summarized in Table 1. The consistency between the predicted and observed values confirmed the robustness of the optimization approach, demonstrating its potential for enhancing substrate accessibility and sugar yield efficiency.

Table 1. Experimental Results at Optimized Conditions Derived from the Model

Error Percentage (%)	Predicted Reducing Sugar Index (Model-Based)	Measured Reducing Sugar Index	Experiment No.
2.1	**1.051**	**1.073**	**1**
0.85	**1.051**	**1.042**	**2**
2.3	**1.051**	**1.027**	**3**
Average Error: 1.75%			

Given the high predictive accuracy of the developed model, a deviation of less than 5% between the predicted and experimental values was considered an acceptable margin of error. This threshold ensures the model's reliability in optimizing the acid hydrolysis process while accounting for minor experimental variations. The close agreement between the predicted and observed reducing sugar indices further validates the model's robustness and applicability in biomass valorization processes.

3.2.2. Model Development for the Reducing Sugar Index

A reduced quadratic model was developed using the Response Surface Methodology (RSM) approach to predict the reducing sugar index. The final model, expressed in coded variables, is presented as follows:

Equation (1): the Reducing Sugar Index Model

$$\mathbf{Y = 0.8168 - 0.0646\ A - 0.0546\ B + 0.0220\ C - 0.1119\ D + 0.06550\ A{\times}B - 0.0341\ A{\times}D - 0.0973\ B \times D - 0.0741\ C \times D - 0.1371\ A^2 + 0.1079\ B^2 - 0.0706\ D^2}$$

where Y represents the reducing sugar index.

Statistical Validation of the Model

The accuracy and significance of the model were assessed using analysis of variance (ANOVA), with the results presented in Table 2. The model demonstrated a strong predictive capability, as evidenced by the high *F*-value (1458.17) and highly significant *p*-values ($p < 0.0001$) for all linear, interaction, and quadratic terms. The non-significant lack-of-fit test ($p = 0.0500$) confirms that the model adequately fits the data, minimizing unexplained variation.

Among the main effects, reaction time (*D*) had the most substantial influence (*SS* = 0.2252, *F* = 4452.60), followed by β value, acid concentration, and temperature. Significant interaction effects were also observed, particularly between acid concentration and time (*BD*, *SS* = 0.1514, *F* =

2993.27) and between temperature and time (*CD*, *SS* = 0.0880, *F* = 1739.25), highlighting complex dependencies within the system.

Model Performance Metrics

The model explained 99.89% of the total variance (*SS_model* = 0.8113, *Cor Total SS* = 0.8122), with excellent fit statistics:

- **R^2** = 0.9989
- **Adjusted R^2** = 0.9982
- **Predicted R^2** = 0.9958
- **Coefficient of Variation (C.V.)** = 0.9396%

Additionally, the high adequate precision value (141.143) confirms a strong signal-to-noise ratio, ensuring the model's reliability for optimization and process improvement. These results collectively demonstrate that the developed model is a robust predictive tool for optimizing the acid hydrolysis process.

Table 2. ANOVA Results for the Reduced Quadratic Model of Reducing Sugar Index

Source	Sum of Squares	df	Mean Square	F-value	p-value	Significance
Model	**0.8113**	**11**	**0.0738**	**1458.17**	**< 0.0001**	**significant**
A-β	**0.0752**	**1**	**0.0752**	**1487.25**	**< 0.0001**	
B-Acid concentration	**0.0538**	**1**	**0.0538**	**1062.71**	**< 0.0001**	
C-Temperature	**0.0087**	**1**	**0.0087**	**172.58**	**< 0.0001**	
D-Time	**0.2252**	**1**	**0.2252**	**4452.60**	**< 0.0001**	
AB	**0.0676**	**1**	**0.0676**	**1337.51**	**< 0.0001**	
AD	**0.0187**	**1**	**0.0187**	**368.90**	**< 0.0001**	
BD	**0.1514**	**1**	**0.1514**	**2993.27**	**< 0.0001**	
CD	**0.0880**	**1**	**0.0880**	**1739.25**	**< 0.0001**	
A^2	**0.0534**	**1**	**0.0534**	**1055.20**	**< 0.0001**	
B^2	**0.0330**	**1**	**0.0330**	**653.23**	**< 0.0001**	
D^2	**0.0142**	**1**	**0.0142**	**279.88**	**< 0.0001**	
Residual	**0.0009**	**18**	**0.0001**			
Lack of Fit	**0.0008**	**13**	**0.0001**	**4.65**	**0.0500**	**not significant**
Pure Error	**0.0001**	**5**	**0.0000**			
Cor Total	**0.8122**	**29**				

3.2.3. Effects of Investigated Factors on Reducing Sugar Index

The interactive effects of temperature, reaction time, acid concentration, and the acid ratio (β) on the reducing sugar index were analyzed to optimize acid hydrolysis conditions for lignocellulosic biomass.

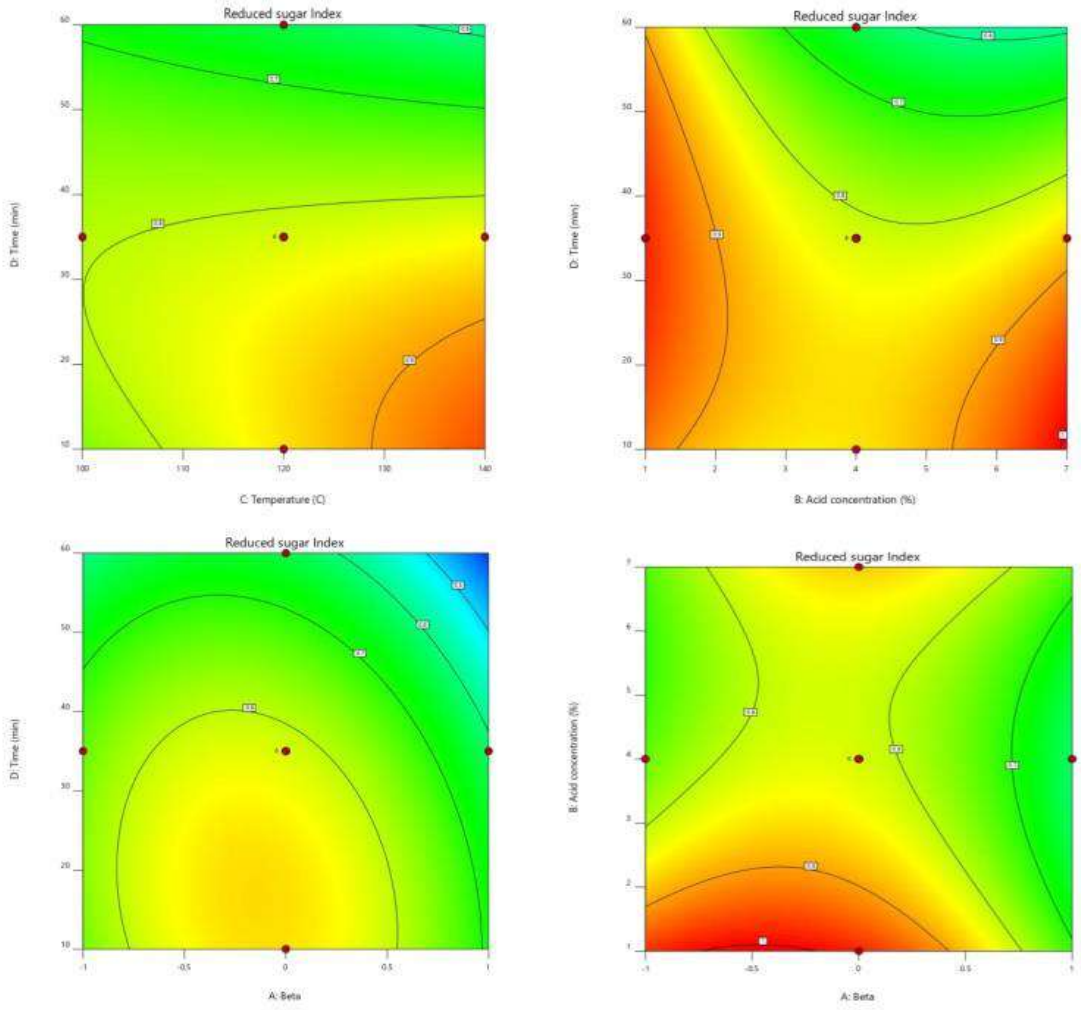

Figure 3. Interaction Effects of Different Factors on reducing sugar index

Figure 3 illustrates the interactive effects of temperature, reaction time, acid concentration, and the acid ratio (β) on the reducing sugar index during acid hydrolysis of lignocellulosic biomass.

Effect of Acid Type and Concentration

The choice of acid played a critical role in hydrolysis efficiency. Sulfuric acid (β = -1) effectively disrupted the crystalline structures of cellulose and hemicellulose, facilitating sugar release. However, at high concentrations, it generated inhibitory byproducts, reducing hydrolysis efficiency. Conversely, nitric acid (β = 1) functioned both as a strong acid and an oxidizing agent, enhancing lignin degradation. However, excessive oxidation led to the formation of nitro-compounds, which negatively impacted sugar yield. A balanced combination of both acids ($\beta \approx 0$) optimized cellulose hydrolysis and lignin removal, resulting in the highest reducing sugar index yield.

Role of Temperature and Reaction Time

Temperature and reaction time significantly influenced sugar release. High temperatures (130–140°C) coupled with short reaction times (10–20 minutes) and moderate acid concentrations (6–

6.8% *w/w*) maximized sugar production while minimizing degradation byproducts. However, prolonged hydrolysis times (>50 minutes) or excessive acid concentrations (>6.8% (w/w)) promoted secondary reactions, leading to sugar degradation and reduced yields.

Optimized Hydrolysis Conditions

The optimal conditions ($\beta \approx 0$, acid concentration: 6–6.8% *w/w*, reaction time: 10–20 minutes) aligned with previous research findings, confirming that a controlled mixture of sulfuric and nitric acids enhances sugar release while minimizing inhibitory byproducts (Veluchamy et al., 2017; Ariunbaatar et al., 2014; Taherzadeh & Karimi, 2007; Rabemanolontsoa, 2016; Rana et al., 2023).

3.3. Optimization of Yeast-Microalgae Co-Cultivation Conditions

A mathematical model was developed to predict lipid yield, carotenoid content, biomass production, and COD removal efficiency during the co-cultivation of *Rhodosporidium babjevae* yeast and *Arthrospira platensis* microalgae. Experimental trials were conducted to validate the optimized conditions identified through model predictions.

3.3.1. Optimized Conditions Based on Model Predictions

The optimized co-cultivation parameters were as follows:

- **Light intensity (D):** 3.8 Klux
- **Airflow rate (C):** 1.4 L/min
- **Cultivation duration (B):** 5.7 days
- **Microalgae-to-yeast ratio (A):** 2.6

Under these conditions, the following responses were achieved:

- **Lipid yield (Y_1):** 6.683 g/L
- **Carotenoid yield (Y_2):** 25.099 mg/L
- **Biomass concentration (Y_3):** 8.659 g/L
- **COD removal efficiency (Y_4):** 86.762%

Experimental Validation

To confirm the reliability of these optimized conditions, three independent co-cultivation experiments were conducted. The results, presented in Table 3, demonstrated strong agreement with model predictions, confirming the robustness of the optimization process.

Table 3. Experimental Validation at Optimized Model Conditions

Error (%) Carotenoid	Error (%) Lipid	Error (%) Biomass	Error (%) COD	Carotenoid Yield (mg/L)	Lipid Yield (g/L)	Biomass Yield (g/L)	COD Removal Efficiency (%)	Test No.
3.58	**1.60**	**1.74**	**0.50**	**26**	**6.79**	**8.81**	**87.2**	**1**
8.36	**4.83**	**2.87**	**1.68**	**23**	**6.36**	**8.41**	**85.3**	**2**
0.39	**2.28**	**1.16**	**0.18**	**25**	**6.53**	**8.76**	**86.6**	**3**

Model Performance Metrics:

- **Average Error for COD Removal Model:** 0.78%

- **Average Error for Biomass Yield Model:** 1.92%
- **Average Error for Lipid Yield Model:** 2.90%
- **Average Error for Carotenoid Yield Model:** 4.11%

These results demonstrate the high accuracy of the optimized model, with all experimental values closely aligning with predicted values. The low percentage errors confirm the model's robustness in optimizing yeast-microalgae co-cultivation conditions for enhanced lipid and carotenoid production, biomass growth, and COD removal efficiency.

3.3.2. Model Extraction for COD Removal Efficiency

Using the RSM, a reduced quadratic model was developed to predict the COD removal efficiency in the co-cultivation system. The final model, expressed in terms of coded variables, is given below, where Y_1 represents the COD removal percentage:

Equation (2): COD Removal Model

$$\mathbf{Y_1 = 82.80 + 5.17\ A + 8.83\ B + 1.17\ C + 0.5\ D + 2.75(A \times B) + 1.75(A \times C) - 2.25(C \times D) - 6.98\ A^2 - 11.98\ B^2 - 0.9833\ C^2 - 5.48\ D^2}$$

Where:

- **A** = Microalgae-to-yeast ratio
- **B** = Cultivation duration
- **C** = Airflow rate
- **D** = Light intensity

This model allows for accurate prediction of COD removal efficiency under different co-cultivation conditions. The corresponding ANOVA results for this quadratic model are presented in the next table:

Table 4. ANOVA Results for the Reduced Quadratic Model of COD Removal Efficiency

Source	Sum of Squares	df	Mean Square	F-value	p-value	Significance
Model	**2501.41**	**11**	**227.40**	**146.52**	**< 0.0001**	**Significant**
A - Microalgae to yeast ratio	**320.33**	**1**	**320.33**	**206.41**	**< 0.0001**	
B - Cultivation time	**936.33**	**1**	**936.33**	**603.32**	**< 0.0001**	
C - Airflow rate	**16.33**	**1**	**16.33**	**10.52**	**0.0048**	
D - Light intensity	**3.00**	**1**	**3.00**	**1.93**	**0.1824**	
AB	**30.25**	**1**	**30.25**	**19.49**	**0.0004**	
AC	**12.25**	**1**	**12.25**	**7.89**	**0.0121**	
CD	**20.25**	**1**	**20.25**	**13.05**	**0.0022**	
A^2	**316.33**	**1**	**316.33**	**203.82**	**< 0.0001**	
B^2	**931.46**	**1**	**931.46**	**600.18**	**< 0.0001**	
C^2	**6.27**	**1**	**6.27**	**4.04**	**0.0605**	

D^2	**195.03**	**1**	**195.03**	**125.67**	**< 0.0001**	
Residual	**26.38**	**17**	**1.55**			
Lack of Fit	**11.58**	**13**	**0.8910**	**0.2408**	**0.9780**	**Not significant**
Pure Error	**14.80**	**4**	**3.70**			
Cor Total	**2527.79**	**28**				

Statistical Validation of the Model

The reliability and predictive accuracy of the model were evaluated using ANOVA, with the results summarized in Table 2. The model exhibited strong statistical significance, as indicated by a high F-value (146.52) and an extremely low p-value ($p < 0.0001$), confirming that the selected factors and their interactions significantly influenced COD removal efficiency. The non-significant lack-of-fit test ($p = 0.9780$) suggests that the model adequately represents the experimental data without substantial unexplained variation.

Among the main effects, cultivation time ($F = 603.32$) had the most pronounced impact, followed by the microalgae-to-yeast ratio ($F = 206.41$) and airflow rate ($F = 10.52$). Several interaction effects were also significant, particularly microalgae-to-yeast ratio × cultivation time (AB, $F = 19.49$) and airflow rate × light intensity (CD, $F = 13.05$), underscoring the complex interdependencies among process variables.

Model Performance Metrics

The model accounted for 98.96% of the total response variation ($SS_{model} = 2501.41$, $SS_{total} = 2527.79$), demonstrating excellent predictive accuracy with the following statistical indicators:

- **R^2 =** 0.9896
- **Adjusted R^2 =** 0.9828
- **Predicted R^2 =** 0.9762
- **Coefficient of Variation (C.V.) =** 1.72%

Furthermore, the high adequate precision value (37.85), well above the acceptable threshold of 4, confirms a strong signal-to-noise ratio, reinforcing the model's robustness for optimization purposes. Collectively, these statistical results validate the model's reliability, predictive strength, and suitability as a powerful tool for optimizing yeast-microalgae co-cultivation conditions to maximize COD removal efficiency.

3.3.2.1. Effects of Investigated Factors on COD Removal Efficiency

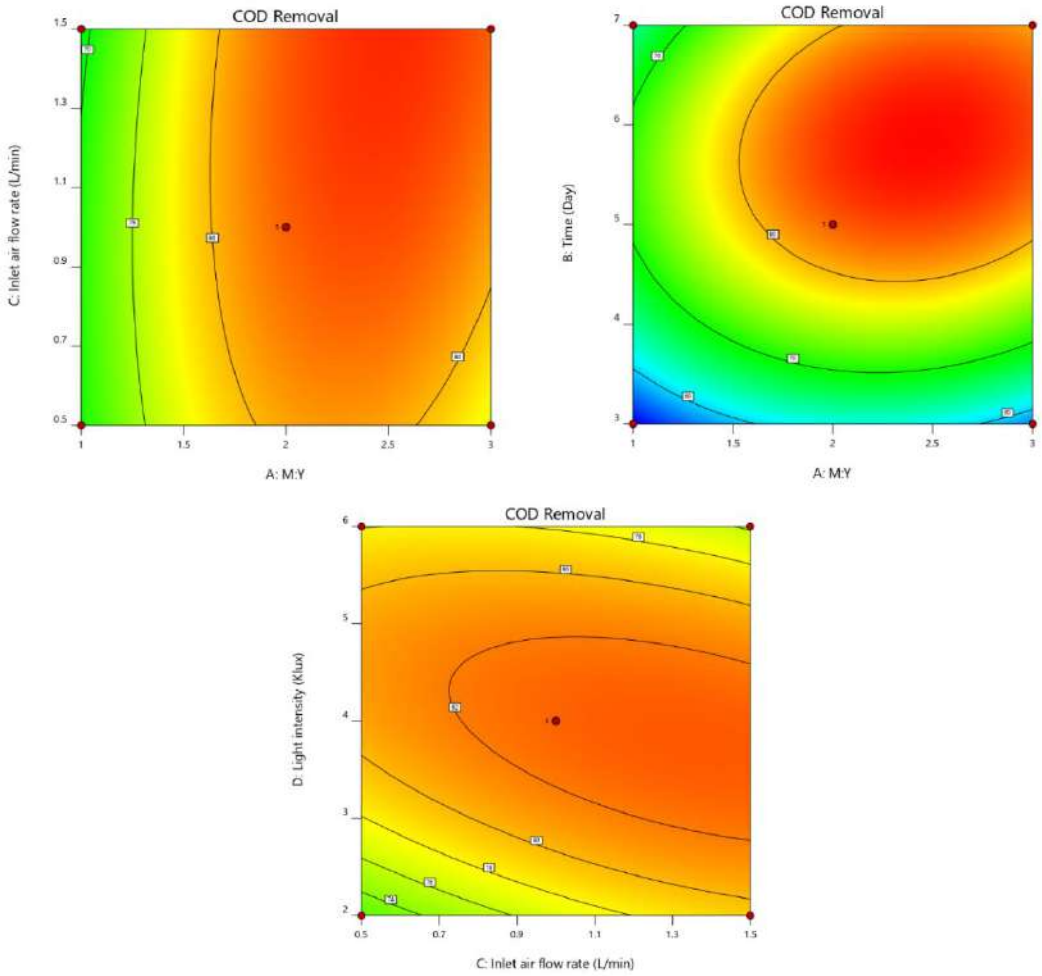

Figure 4. Interaction Effects of Different Factors on COD Removal Efficiency

Figure 4 shows that major operational factors such as light intensity, airflow rate, cultivation period, and algae-to-yeast ratio have a substantial impact on COD removal efficiency in the co-culture system of Arthrospira platensis and Rhodosporidium babjevae. The combination of *A. platensis's* oxygen generation and *R. babjevae's* organic matter breakdown is critical for COD elimination. Optimal light intensity promotes oxygen evolution, yeast metabolism, and pollutant breakdown, whereas low or excessive light decreases efficiency (Banerjee et al., 2016; Cheirsilp et al., 2011; Kitcha & Cheirsilp, 2014; Wahidin et al., 2013; Huo et al., 2011; Zhang et al., 2024; Ugya et al., 2024). An airflow rate of 1.4 L/min enhances gas exchange and aeration, which promotes yeast activity (Kitcha and Cheirsilp, 2014; Wahidin et al., 2013). A 5.7-day culture time maximizes microbial efficiency, however longer periods may impair efficacy (Banerjee et al., 2016; Zhang et al., 2024). The algae-to-yeast ratio of 2.6 preserves oxygen balance, limiting yeast overgrowth, which might impede COD removal (Cheirsilp et al., 2011; Kitcha and Cheirsilp, 2014).

With these modifications, the system obtained 86.762% COD removal, demonstrating its potential for wastewater treatment (Ugya et al., 2024).

3.3.3. Development of the Predictive Model for Carotenoid Yield

Utilizing the RSM, a reduced quadratic model was formulated to predict carotenoid extraction efficiency with high accuracy. This final model, expressed in terms of coded variables, defines carotenoid yield (Y_2) as the response variable, incorporating both linear and interaction effects to capture the underlying process dynamics.

Equation (3): Carotenoid Yield Model

$$\mathbf{Y_2 = 23.03 + 1.83\ A + 4.42\ B + 1.17\ C + 1.42\ D + 1.25(A \times D) - (B \times D) - 2.5(C \times D) - 2.47\ A^2 - 4.34\ B^2 - 3.34\ D^2}$$

The statistical significance and reliability of this model were further validated through ANOVA, with the detailed results summarized in the following table.

Table 5. Analysis of Variance for the Reduced Quadratic Model of Carotenoid Yield

Source	Sum of Squares (SS)	df	Mean Square (MS)	F-value	p-value	Significance
Model	**539.38**	**10**	**53.94**	**143.59**	**< 0.0001**	**Significant**
A - Microalgae-to-Yeast Ratio	**40.33**	**1**	**40.33**	**107.38**	**< 0.0001**	
B - Cultivation Time	**234.08**	**1**	**234.08**	**623.18**	**< 0.0001**	
C - Aeration Rate	**16.33**	**1**	**16.33**	**43.48**	**< 0.0001**	
D - Light Intensity	**24.08**	**1**	**24.08**	**64.12**	**< 0.0001**	
AD	**6.25**	**1**	**6.25**	**16.64**	**0.0007**	
BD	**4.00**	**1**	**4.00**	**10.65**	**0.0043**	
CD	**25.00**	**1**	**25.00**	**66.56**	**< 0.0001**	
A^2	**40.92**	**1**	**40.92**	**108.93**	**< 0.0001**	
B^2	**126.78**	**1**	**126.78**	**337.53**	**< 0.0001**	
D^2	**75.10**	**1**	**75.10**	**199.94**	**< 0.0001**	
Residual	**6.76**	**18**	**0.3756**	**-**	**-**	
Lack of Fit	**5.96**	**14**	**0.4258**	**2.13**	**0.2428**	**Not significant**
Pure Error	**0.8000**	**4**	**0.2000**	**-**	**-**	
Total	**546.14**	**28**	**-**	**-**	**-**	

Statistical Validation of the Model & Model Performance Metrics

The reduced quadratic model for carotenoid extraction yield demonstrates high statistical significance, with a very high F-value (143.59) and an extremely low p-value (<0.0001), confirming its predictive power. The total sum of squares (SS = 539.38) shows that the independent variables account for most of the observed variability. Cultivation time (SS = 234.08, F = 623.18, $p < 0.0001$) emerged as the most significant factor, followed by the algal-to-yeast ratio (SS = 40.33,

F = 107.38, p < 0.0001), aeration rate (SS = 16.33, F = 43.48, p < 0.0001), and light intensity (SS = 24.08, F = 64.12, p < 0.0001). Significant interaction effects, especially between aeration rate and light intensity (F = 66.56, p < 0.0001), point to key interdependencies that should be factored into optimization. The quadratic terms for all critical factors highlight the importance of precise optimization to capture nonlinear relationships. The minimal residual error (SS = 6.76) and strong goodness-of-fit metrics—R^2 = 0.9876, adjusted R^2 = 0.9807, predicted R^2 = 0.9651—demonstrate excellent model accuracy. A high adequate precision ratio (41.75) further confirms the model's robustness, making it a reliable tool for optimization in real-world applications.

3.3.3.1 Effects of Investigated Factors on Carotenoid Extraction Yield

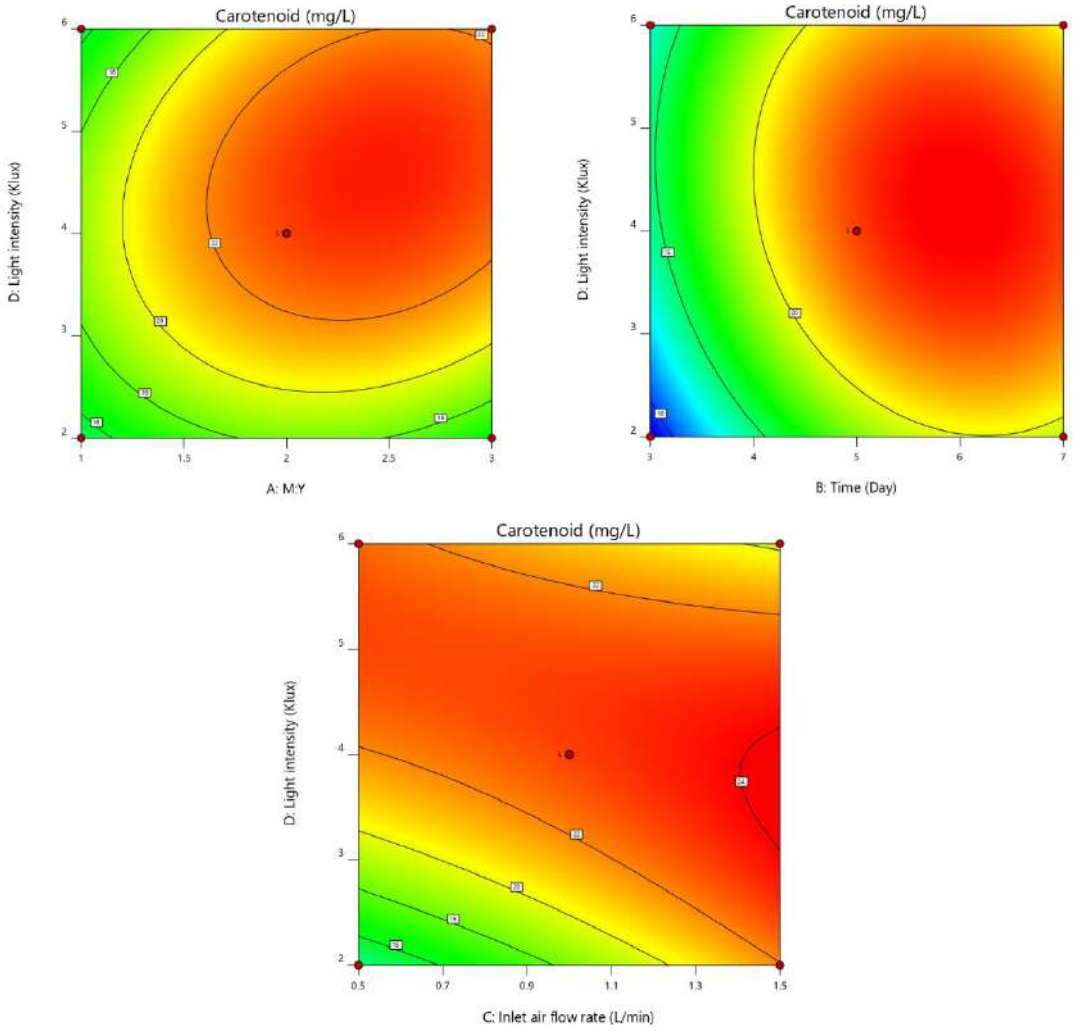

Figure 5. Interaction Effects of Different Factors on Carotenoid Extraction Yield

Carotenoid production in the R. babjevae-A. platensis co-culture is affected by light intensity, cultivation period, aeration rate, and microalga-to-yeast ratio. Optimal light (3.8 Klux) balances ROS levels and promotes biosynthesis, but low or excessive light impairs metabolic processes (Cheirsilp et al., 2011; Kitcha & Cheirsilp, 2014; Wahidin et al., 2013; Gao et al., 2021; Huo et al., 2011; Varela et al., 2015).

A 5.7-day culture time improves enzyme performance while preventing nutrient depletion and ROS-induced degradation (Landolfo et al., 2018). Proper aeration (1.4 L/min) provides oxygen without producing mechanical stress (Ren et al., 2022; Prabhu et al., 2024). A 2.6:1 microalga-to-yeast ratio promotes metabolic balance and prevents resource rivalry (Sforza et al., 2018; Mathew et al., 2022).

Interactions between these parameters, such as light and aeration, culture period, and resource availability, have an additional influence on carotenoid production (Varela et al., 2015).

Thus, optimizing these interdependent variables collectively enhances metabolic efficiency and ensures maximal carotenoid accumulation, underscoring the importance of a well-balanced co-culture system for improved bioprocess performance.

3.3.4. Model Development for Lipid Yield Prediction

Using the RSM approach, a reduced quadratic model was established to accurately predict lipid yield. The final model, expressed in terms of coded variables, represents lipid yield (Y_3) as the response variable:

Equation (4): Lipid Yield Prediction Model

$$Y_3 = 6.31 + 0.0650\,A + 1.24\,B + 0.1817\,C + 0.1950\,D + 0.3575(A\times C) + 0.46(A\times D) - 0.57(C\times D) - 0.4226\,A^2 - 1.32\,B^2 - 0.1276\,C^2 - 0.4901\,D^2$$

This predictive model integrates the primary factors, their interaction effects, and quadratic terms to capture both linear and nonlinear influences on lipid biosynthesis. The significance and reliability of the model were further evaluated using analysis of variance, as detailed in the following table.

Table 6. Analysis of Variance for the Reduced Quadratic Model of Lipid Yield

Source	Sum of Squares	df	Mean Square	F-value	p-value	Significance
Model	**34.14**	**11**	**3.10**	**204.30**	**< 0.0001**	**significant**
A - Microalgae-to-Yeast Ratio	**0.0507**	**1**	**0.0507**	**3.34**	**0.0854**	
B - Cultivation Time	**18.50**	**1**	**18.50**	**1217.69**	**< 0.0001**	
C - Aeration Rate	**0.3960**	**1**	**0.3960**	**26.07**	**< 0.0001**	
D - Light Intensity	**0.4563**	**1**	**0.4563**	**30.03**	**< 0.0001**	
AC	**0.5112**	**1**	**0.5112**	**33.65**	**< 0.0001**	
AD	**0.8464**	**1**	**0.8464**	**55.71**	**< 0.0001**	
CD	**1.30**	**1**	**1.30**	**85.54**	**< 0.0001**	
A^2	**1.16**	**1**	**1.16**	**76.24**	**< 0.0001**	
B^2	**11.35**	**1**	**11.35**	**746.80**	**< 0.0001**	
C^2	**0.1056**	**1**	**0.1056**	**6.95**	**0.0173**	
D^2	**1.56**	**1**	**1.56**	**102.54**	**< 0.0001**	
Residual	**0.2583**	**17**	**0.0152**			

Lack of Fit	**0.2370**	**13**	**0.0182**	**3.42**	**0.1223**	**not significant**
Pure Error	**0.0213**	**4**	**0.0053**			
Cor Total	**34.40**	**28**				

Statistical Validation of the Model & Model Performance Metrics

The reduced quadratic model demonstrated strong predictive accuracy for lipid production, explaining 99.25% of the total variation ($R^2 = 0.9925$). Its statistical robustness was supported by a high F-value of 204.30 ($p < 0.0001$). Among the factors, cultivation time had the most significant impact on lipid yield ($F = 1217.69$, $p < 0.0001$), followed by light intensity ($F = 30.03$, $p < 0.0001$) and airflow rate ($F = 26.07$, $p < 0.0001$). Notable interaction effects were found between light intensity and airflow rate ($F = 85.54$, $p < 0.0001$), as well as between the microalgae-to-yeast ratio and airflow rate ($F = 33.65$, $p < 0.0001$) and light intensity ($F = 55.71$, $p < 0.0001$). The model also exhibited a high predicted R^2 (0.9728) and a precision ratio of 41.661, confirming its suitability for process optimization. The low coefficient of variation (C.V. = 2.31%) and standard deviation (SD = 0.1233) indicated minimal experimental variability, while the non-significant lack-of-fit test ($p = 0.1223$) further confirmed the model's adequacy. These results validate the model's reliability and accuracy for predicting lipid production.

3.3.4.1. Effects of Key Factors on Lipid Yield

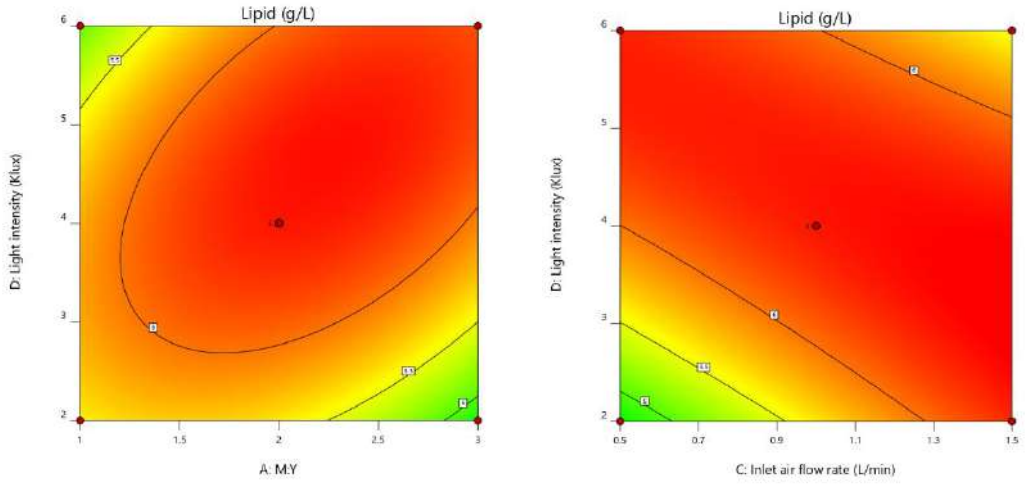

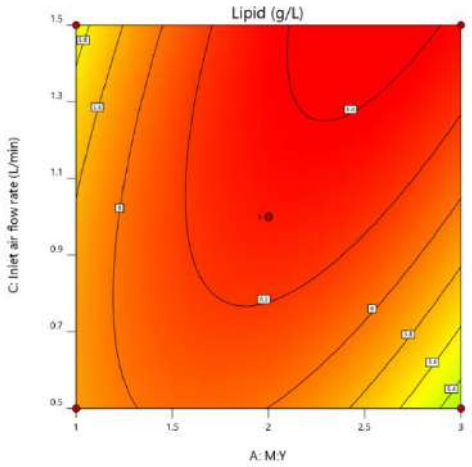

Figure 6. Interaction Effects of Different Factors on Lipid Yield

Interactive Influence of Environmental Parameters

The lipid yield is optimized based on growing duration, microalgae-to-yeast ratio, light intensity, and aeration rate. The TCA cycle promotes lipid production, with acetyl-CoA serving as a major precursor. Optimal aeration (1.4 L/min) promotes steady acetyl-CoA synthesis, but insufficient oxygen disturbs metabolism and excessive aeration produces cellular stress (Shtaida et al., 2015; An et al., 2024).

The Calvin cycle promotes CO_2 fixation and lipid precursor production. At 3.8 Klux, ATP and NADPH production are balanced, but low light restricts energy supply, while high light promotes ROS damage (Xiao et al., 2020; Voon et al., 2021). Cultivation time of less than 5.7 days emphasizes biomass growth, whereas longer durations deplete nutrients and reduce lipid production.

Regulation of Lipid Biosynthesis by Enzymatic Activity

Lipid biosynthesis is tightly regulated by key metabolic enzymes (Satoh et al., 2020; Cronan et al., 2021). ACC catalyzes the conversion of acetyl-CoA to malonyl-CoA, marking the initial step in fatty acid synthesis. Under optimal aeration and light conditions, ACC activity reaches its peak; however, it declines under photonic or mechanical stress. FAS mediates fatty acid chain elongation, a process that relies on NADPH generated from both the Calvin cycle and the pentose phosphate pathway (PPP). In conditions of low light or short cultivation durations, NADPH availability becomes insufficient, thereby constraining FAS activity. Additionally, prolonged cultivation beyond 5.7 days induces the upregulation of lipases and peroxidases, leading to triglyceride hydrolysis and a subsequent reduction in lipid yield.

Impact of Microalgae-to-Yeast Ratio on Metabolic Interactions

The microalgae-to-yeast ratio plays a crucial role in shaping metabolic interactions (Cui et al., 2019). Yeast respiration generates CO_2, which supports microalgal photosynthesis, while microalgae provide oxygen for aerobic respiration in yeast. The optimal ratio of 2.6:1 ensures a balanced metabolic exchange. At lower ratios, yeast dominance leads to rapid nutrient depletion, whereas higher ratios intensify competition for carbon and nitrogen sources, suppressing lipid

production. Both microorganisms utilize glycolysis and the TCA cycle to generate acetyl-CoA and NADPH; however, an imbalance in their ratio diverts metabolic flux toward alternative pathways (e.g., protein or carotenoid synthesis), reducing lipid accumulation.

Optimization of Environmental Conditions for Lipid Biosynthesis

Optimizing environmental parameters is essential for the coordinated metabolic activity of the TCA cycle, Calvin cycle, and lipid biosynthetic pathways. Metabolic balance maximizes ATP, NADPH, and lipid precursor production, whereas deviations disrupt biosynthetic efficiency, leading to reduced lipid yield. The synergistic effects of cultivation parameters significantly impact lipid production (Lee et al., 2016).

- **Interaction of Light Intensity and Cultivation Time (D × B):** Under low light (2 Klux) and short cultivation (3 days), ATP and NADPH limitations restrict CO_2 fixation and lipid synthesis. Additionally, yeast undergoes anaerobic respiration due to insufficient oxygen supply. At excessive light exposure (6 Klux) and extended cultivation (7 days), ROS accumulation induces oxidative stress, leading to lipid peroxidation and reduced lipid yield. The optimal condition (3.8 Klux, 5.7 days) ensures balanced ATP and NADPH production, sustaining CO_2 fixation and lipid biosynthesis.
- **Interaction of Aeration and Microalgae-to-Yeast Ratio (C × A):** At low aeration (0.5 L/min) and a low microalgae-to-yeast ratio (1:1), oxygen deficiency shifts yeast metabolism toward fermentation, reducing lipid synthesis. Simultaneously, limited CO_2 availability restricts microalgal photosynthesis. At high aeration (1.5 L/min) and a high microalgae-to-yeast ratio (3:1), mechanical stress disrupts cellular membranes, while excessive microalgal density intensifies nutrient competition, suppressing yeast growth. The optimal conditions (1.4 L/min, 2.6:1) facilitate efficient oxygen and CO_2 exchange, enhancing lipid biosynthesis.
- **Interaction of Light Intensity and Aeration (D × C):** At low light (2 Klux) and low aeration (0.5 L/min), NADPH and ATP generation are restricted, limiting lipid biosynthesis. Conversely, high light (6 Klux) and high aeration (1.5 L/min) promote ROS formation and cellular stress. The optimal combination (3.8 Klux, 1.4 L/min) synchronizes photosynthetic energy production with aerobic respiration, maximizing lipid yield.
- **Interaction of Cultivation Time and Microalgae-to-Yeast Ratio (B × A):** Under short cultivation (3 days) and low microalgae-to-yeast ratio (1:1), yeast rapidly depletes available nutrients before significant lipid accumulation occurs. On the other hand, extended cultivation (7 days) and a high ratio (3:1) result in excessive lipid peroxidation and nutrient limitation, ultimately suppressing yeast growth. The optimal condition (5.7 days, 2.6:1) maintains synchronized metabolic activity, ensuring efficient nutrient utilization and oxygen exchange for lipid synthesis.

Achieving metabolic coordination across glycolysis, the TCA cycle, the Calvin cycle, and lipid biosynthetic pathways is essential for maximizing lipid yield in yeast-microalgae co-cultures. Aeration and microalgae-to-yeast ratio regulate oxygen and CO_2 availability, influencing TCA cycle efficiency and ATP production. Light intensity and cultivation time determine NADPH and

G3P availability, which directly control fatty acid biosynthesis. However, excessive aeration or illumination disturbs redox homeostasis, leading to ROS accumulation and lipid degradation (Xiao et al., 2020). By fine-tuning environmental parameters, a metabolically balanced state can be achieved, ensuring maximum lipid accumulation and enhanced co-culture productivity.

3.3.5. Predictive Modeling for Biomass Production

A reduced quadratic model was formulated using RSM to estimate biomass production efficiency. The final model, expressed in terms of coded variables, represents the biomass yield (Y_4) as follows:

Equation (5): Biomass Production Model

$$Y_4 = 8.25 + 0.2483\,A + 1.73\,B + 0.1475\,C + 0.0650\,D + 0.2325(A \times C) - 0.2025(C \times D) - 0.5636\,A^2 - 1.43\,B^2 - 0.3048\,C^2 - 0.4361\,D^2$$

To evaluate the reliability and accuracy of this model, an ANOVA was conducted (Table 7).

Table 7. ANOVA for the reduced quadratic model for biomass yield

Source	Sum of Squares	df	Mean Square	F-value	p-value	Significance
Model	**51.14**	**10**	**5.11**	**244.45**	**< 0.0001**	**significant**
A - Microalgae-to-yeast ratio	**0.7400**	**1**	**0.7400**	**35.37**	**< 0.0001**	
B - Cultivation time	**35.81**	**1**	**35.81**	**1711.72**	**< 0.0001**	
C - Airflow rate	**0.2611**	**1**	**0.2611**	**12.48**	**0.0024**	
D - Light intensity	**0.0507**	**1**	**0.0507**	**2.42**	**0.1369**	
AC	**0.2162**	**1**	**0.2162**	**10.34**	**0.0048**	
CD	**0.1640**	**1**	**0.1640**	**7.84**	**0.0118**	
A^2	**2.06**	**1**	**2.06**	**98.48**	**< 0.0001**	
B^2	**13.21**	**1**	**13.21**	**631.65**	**< 0.0001**	
C^2	**0.6027**	**1**	**0.6027**	**28.81**	**< 0.0001**	
D^2	**1.23**	**1**	**1.23**	**58.96**	**< 0.0001**	
Residual	**0.3766**	**18**	**0.0209**			
Lack of Fit	**0.3313**	**14**	**0.0237**	**2.09**	**0.2488**	**not significant**
Pure Error	**0.0453**	**4**	**0.0113**			
Cor Total	**51.52**	**28**				

Statistical Validation of the Model & Model Performance Metrics

The ANOVA findings corroborate the model's resilience, with a high F-value (244.45) and a low p-value (<0.0001), indicating its good predictive power. Cultivation period (B) had the most influence on biomass output, followed by microalgae-to-yeast ratio (A) and airflow rate (C), all with statistical significance ($p < 0.05$). Light intensity (D) had no significant influence ($p = 0.1369$). Significant interaction effects were seen between the microalgae-to-yeast ratio and airflow rate ($F = 10.34$, $p = 0.0048$), as well as between airflow rate and light intensity ($F = 7.84$,

p = 0.0118), emphasizing the significance of optimizing numerous parameters at once. Quadratic effects were also highly significant ($p < 0.0001$), with cultivation time (B^2) showing the strongest curvature ($F = 631.65$). The model's low residual sum of squares (0.3766) indicates minimal unexplained variation. With excellent goodness-of-fit metrics, including R^2 (0.9927) and adjusted R^2 (0.9886), the model proves to be a reliable tool for optimizing biomass production in microalgae-yeast co-cultures. It provides precise guidance for environmental control to maximize productivity.

3.3.5.1. Influence of Key Environmental Factors on Biomass Production

Biomass production in the co-culture of *Rhodosporidium babjevae* and *Arthrospira platensis* is intricately influenced by environmental factors such as light intensity, aeration, and the microalgae-to-yeast ratio. These factors work together to sustain metabolic efficiency and ensure optimal growth. The optimal light intensity of 3.8 Klux supports photosynthesis, facilitating the production of ATP and NADPH, which are essential for the Calvin cycle and biomass synthesis. However, insufficient light limits carbon fixation, while excessive light can lead to reactive oxygen species (ROS) accumulation, inducing oxidative stress. The cultivation period of 5.7 days strikes a balance between growth and nutrient availability, supporting effective enzyme activity for polysaccharide and protein biosynthesis. Aeration at 1.4 L/min ensures adequate oxygen supply for respiration, which is vital for energy production through processes like the TCA cycle. Maintaining a microalgae-to-yeast ratio of 2.6:1 enhances nutrient and gas exchange, reducing competition and promoting symbiosis. Deviations from these optimal conditions can disrupt metabolic pathways, ultimately decreasing biomass yield. These findings emphasize the importance of precise environmental control in optimizing co-culture systems for biotechnological applications, highlighting the potential for innovation in sustainable production processes (Burlacot et al., 2023; Gao et al., 2021; Ye et al., 2018; Abu-Ghosh et al., 2016).

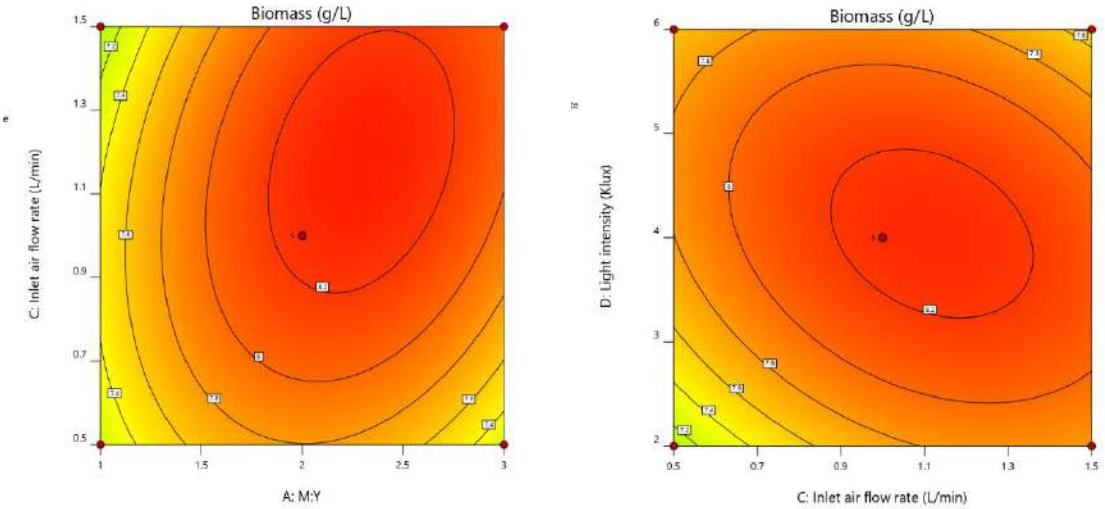

Figure 7. Interaction Effects of Different Factors on Biomass Production

3.4. Comparison of Co-Cultivation and Pure Culture Conditions

Figure 8 illustrates the carotenoid yield obtained from the co-culture of *Rhodosporidium babjevae* yeast and *Arthrospira platensis* microalga, compared to their respective monocultures.

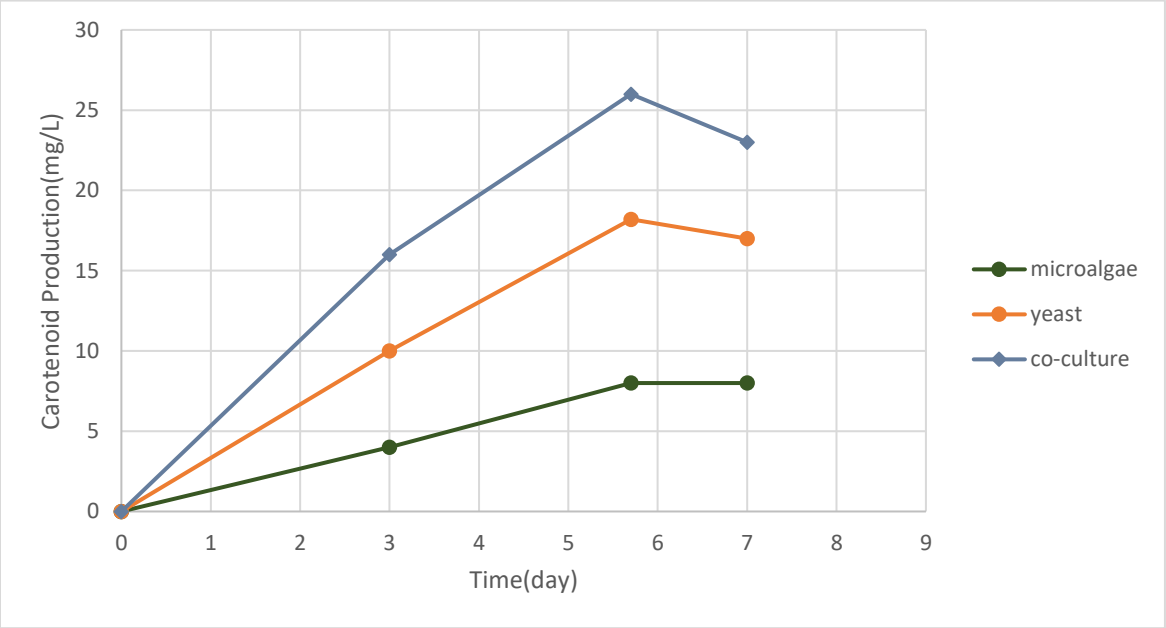

Figure 8. Carotenoid Yield in Co-Culture vs. Pure Culture Conditions

The co-cultivation system led to a substantial increase in carotenoid production, with enhancements of 42.85% and 225% for *R. babjevae* and *A. platensis*, respectively. This remarkable synergistic effect can be attributed to several key mechanisms:

(i) **Nutritional Interactions**: The microalga contributes organic carbon sources (e.g., glucose) through photosynthesis while simultaneously releasing oxygen, which enhances yeast respiration and ATP/NADPH generation—critical components for carotenoid biosynthesis (Pan-Utai et al., 2022; Kato et al., 2021). Conversely, the yeast supplies CO_2 and growth-stimulating compounds, improving microalgal photosynthetic efficiency and metabolic activity.

(ii) **Biochemical Enhancement**: The co-culture system activates key metabolic pathways involved in carotenoid biosynthesis. In yeast, the mevalonate (MVA) pathway is upregulated, while in microalgae, the DOXP/MEP pathway is enhanced, leading to increased synthesis of isoprenoid precursors (Shaker et al., 2021). Gene expression studies confirm the upregulation of carotenogenic genes such as *crtB* and *crtI*, along with higher enzymatic activity related to carotenoid production.

(iii) **Protective Mechanisms**: The co-culture environment induces a mild oxidative stress response, triggering carotenoid accumulation as an adaptive antioxidant defense. This response mitigates ROS-mediated damage and enhances photoprotection, further supporting cellular resilience and metabolic stability (Tamaki et al., 2021).

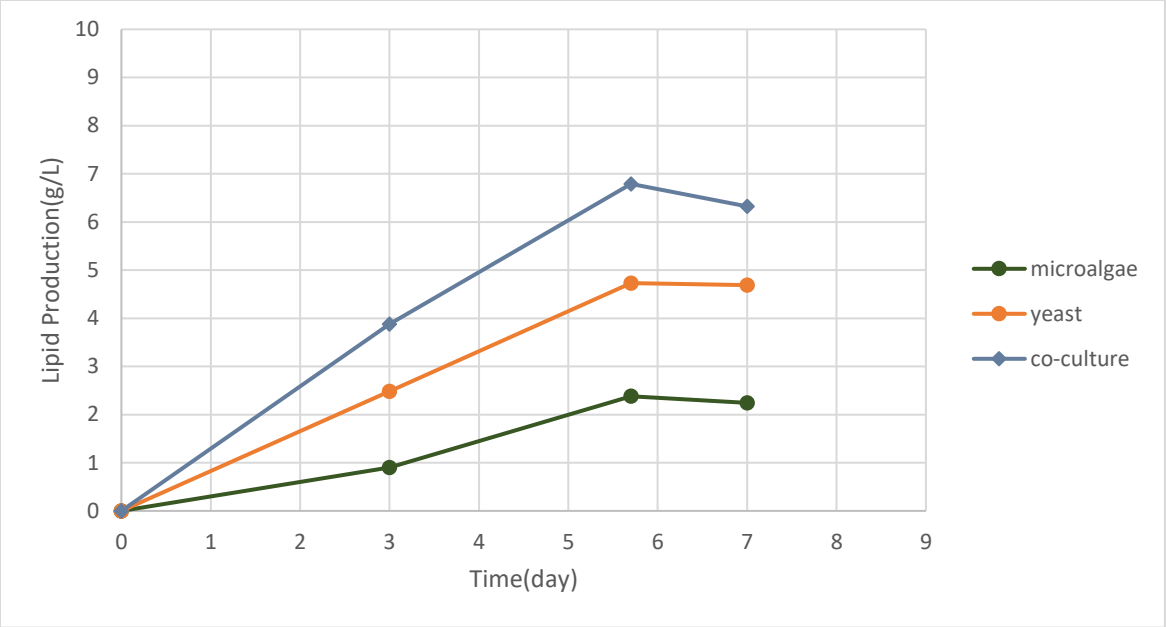

Figure 9. Lipid Yield from Co-Culture and Pure Culture of Yeast and Microalgae

Figure 9 illustrates the lipid yield obtained from the co-culture of *Rhodosporidium babjevae* yeast and *Arthrospira platensis* microalgae, compared to their respective monocultures. The results indicate a substantial enhancement in lipid production under co-cultivation, with lipid yields increasing by 43.55% and 185.29% compared to pure yeast and microalgal cultures, respectively. This improvement can be attributed to several key factors:

(i) Metabolic Interactions and Nutrient Exchange

The microalga promotes lipid formation by providing yeast with carbohydrates (e.g., glucose, sucrose) via photosynthesis, which acts as an extra carbon source. This increases the availability of acetyl-CoA and NADPH, two important precursors for lipid biosynthesis (Qiao et al., 2017). Furthermore, oxygen produced by the microalga stimulates yeast respiration and TCA cycle activity, resulting in increased ATP and acetyl-CoA production. The yeast creates CO_2, which promotes the Calvin cycle in microalgae, boosting NADPH regeneration and improving lipid biosynthesis (Xin et al., 2024). Furthermore, yeast produces important vitamins (e.g., B vitamins) and cofactors that enhance lipid metabolism in microalgae.

(ii) Regulation of Biochemical Pathways

In yeast, the uptake of microalgal-derived glucose intensifies glycolytic flux, leading to increased acetyl-CoA and NADPH levels. This fuels lipid synthesis via the MVA pathway, activating key enzymes such as ACC and FAS, which promote fatty acid chain elongation (Przygrodzka et al., 2024; Chen et al., 2016). In microalgae, the elevated CO_2 levels upregulate Calvin cycle activity, resulting in higher ATP and NADPH production, both of which directly support triglyceride (TAG) biosynthesis. Gene expression analyses further confirm the upregulation of key lipid biosynthetic genes.

(iii) Cellular and Biochemical Adaptations

The co-culture environment causes moderate oxidative stress, which acts as a signal for lipid accumulation in microalgae. Meanwhile, yeast benefits from improved fatty acid metabolism, which results in higher generation of unsaturated fatty acids, improving membrane stability and metabolic efficiency. NADPH, a key cofactor in fatty acid production, is activated by the pentose phosphate cycle and photosynthesis. Furthermore, increasing oxygen availability in co-culture stimulates yeast TCA cycle activity, resulting in more metabolic precursors for lipid biosynthesis (Sun et al., 2019).

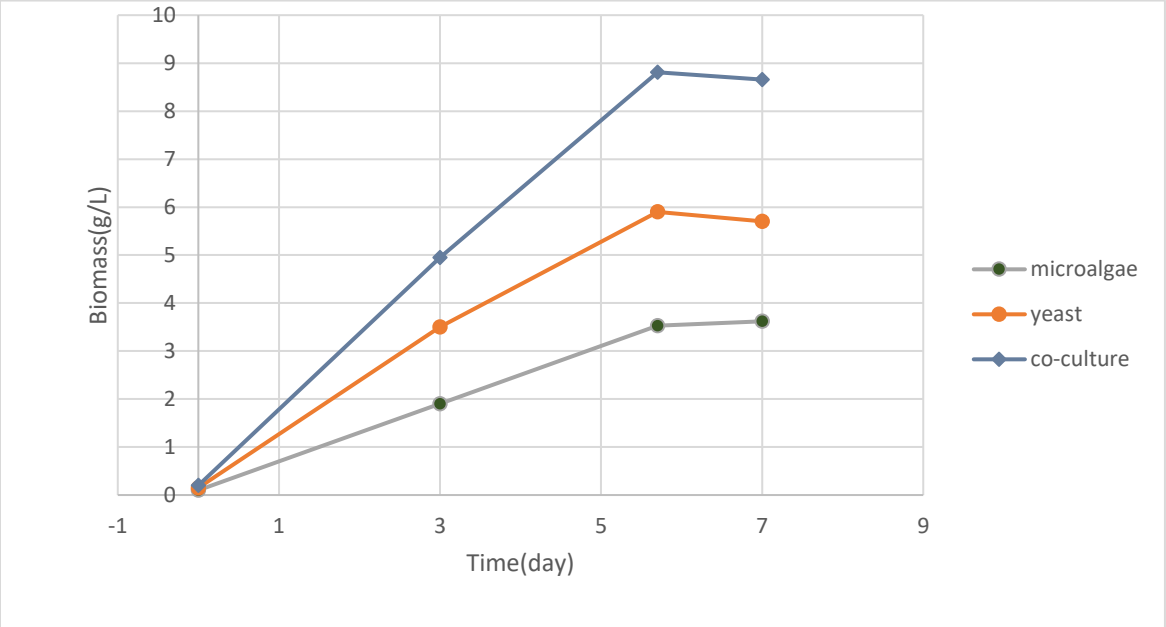

Figure 10. Biomass Yield in Co-Culture and Pure Culture of Yeast and Microalgae

Figure 10 illustrates that the co-culture of *Rhodosporidium babjevae* yeast and *Arthrospira platensis* microalgae results in significantly higher biomass production compared to their monocultures, with increases of 49.32% and 149.57%, respectively. This improvement is attributed to the synergistic nutrient exchange, metabolic regulation, and optimized growth dynamics within the co-culture. The microalgae support yeast growth by supplying oxygen for aerobic respiration and organic carbon sources like glucose, which enhance yeast metabolism (Burlacot et al., 2019; Munch et al., 2015). In turn, the yeast contributes by releasing CO_2, which stimulates the Calvin cycle in the microalgae. Additionally, the yeast secretes growth factors such as B vitamins and amino acids, which support microalgal metabolism and biomass accumulation. Metabolically, the co-culture optimizes ATP production in yeast and promotes rapid microalgal cell proliferation through enhanced CO_2 flux and NADPH production. Gene upregulation in both organisms foster cell division and more efficient energy use. While pure microalgal cultures face limitations due to photosynthetic efficiency and nutrient availability, the co-culture boosts growth in the early cultivation phases by improving nutrient flow. However, prolonged cultivation leads to competition for nitrogen and phosphorus, which can inhibit further growth (Shen et al., 2022).

Figure 11 presents the COD reduction efficiencies observed in the co-culture of *Rhodosporidium babjevae* yeast and *Arthrospira platensis* microalgae, as well as in their respective monocultures.

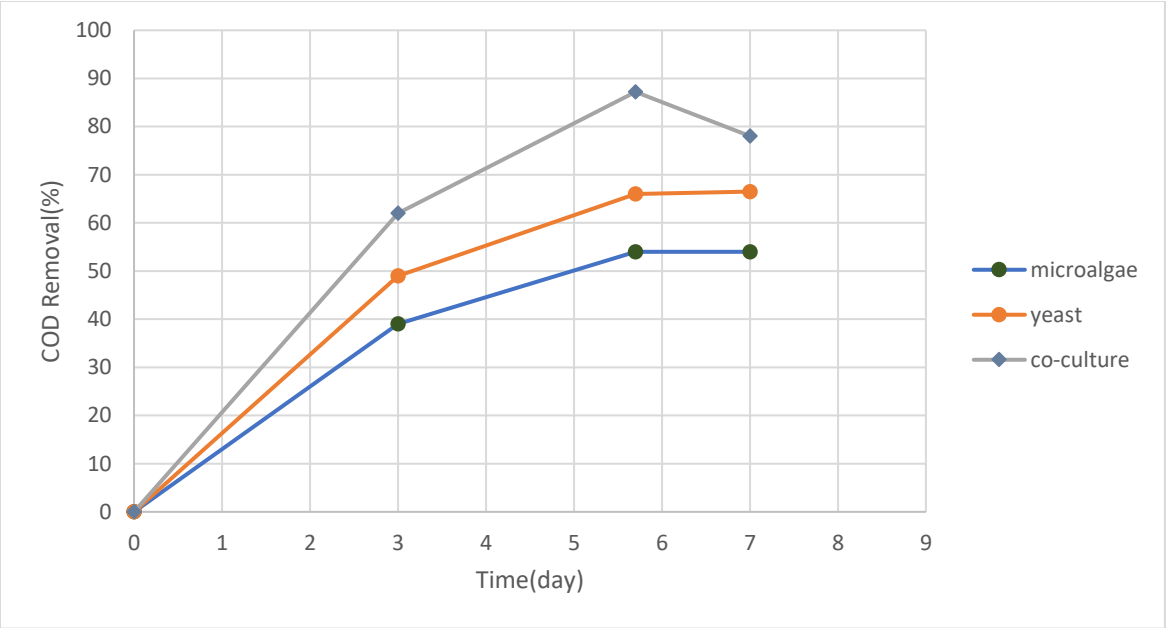

Figure 11. COD Removal Percentage in Co-Culture and Pure Culture of Yeast and Microalgae

The COD removal rate in the Rhodosporidium babjevae-Arthrospira platensis co-culture was 32.12% and 61.48% higher than in pure yeast and microalgal cultures, respectively. This combination increases oxygen generation for yeast respiration and speeds organic matter breakdown via enzymes such as glucose oxidase and catalase (Wang et al., 2018). Yeast secretes enzymes that break down complex compounds, and its CO_2 release stimulates the Calvin cycle in microalgae, leading to better pollutant degradation. COD removal decreases after 5.7 days owing to substrate depletion and metabolic byproduct buildup, although resource exchange maintains efficiency (Tongc et al., 2024; Roy et al., 2023; Mathew et al., 2022).

3.5. Prediction of Physicochemical Properties of Biodiesel Based on Fatty Acid Profiles

The FAME composition of biodiesel derived from the co-culture system, as well as from pure cultures of *Rhodosporidium babjevae* yeast and *Arthrospira platensis* microalgae, is summarized in Table 8.

Table 8. FAME Profiles of Co-Culture and Pure Cultures

Fatty Acid	Yeast Profile (wt/wt%)	Microalgae Profile (wt/wt%)	Co-culture Profile (wt/wt%)
Capric acid (C10:0)	**0.6**	**0.4**	**0.5**
Lauric acid (C12:0)	**0.7**	**0.3**	**0.6**
Myristic acid (C14:0)	**1.4**	**1.4**	**1.8**
Pentadecanoic acid (C15:0)	**1.8**	**1.1**	**1.6**

Palmitic acid (C16:0)	**19**	**50.6**	**31**
Palmitoleic acid (C16:1)	**0.6**	**3.2**	**1.3**
Heptadecanoic acid (C17:0)	**1.7**	**1.2**	**1.5**
Stearic acid (C18:0)	**7**	**1.3**	**5.1**
Oleic acid (C18:1)	**49**	**7**	**33**
Linoleic acid (C18:2)	**10**	**16**	**12**
Linolenic acid (C18:3)	**2.5**	**12**	**3.4**
Unspecified	**5.7**	**5.5**	**8.2**

The fatty acid profile of biodiesel plays a pivotal role in determining its physicochemical properties, such as CFPP, viscosity, oxidative stability, and lubricity, all of which directly impact engine performance, storage stability, and environmental footprint. Saturated fatty acids, like palmitic acid (C16:0) and stearic acid (C18:0), raise CFPP due to their tendency to crystallize, which causes biodiesel to solidify at lower temperatures. On the other hand, unsaturated fatty acids, such as oleic acid (C18:1) and linoleic acid (C18:2), improve cold-flow properties by inhibiting the formation of crystalline structures (Bouaid et al., 2024). The biodiesel produced from the co-culture, rich in oleic acid (33%), demonstrates excellent oxidative stability, prolonging shelf life by resisting degradation, in contrast to polyunsaturated fatty acids like linoleic and linolenic acids. While the latter enhance fluidity and combustion efficiency, they are more susceptible to oxidation (Matsui et al., 2018). The co-culture system also optimizes palmitic acid (31%) content, increasing CFPP and potentially influencing biodiesel performance in cold temperatures, while reducing short-chain fatty acids, which could slightly compromise cold-weather performance (Godoy et al., 2015). The viscosity of the biodiesel is also influenced by fatty acid composition; the presence of oleic acid lowers viscosity, thus enhancing fuel fluidity and atomization in engines (Daels et al., 2020). This carefully balanced fatty acid profile highlights the potential of yeast-microalgae co-cultivation for producing biodiesel that combines enhanced performance, stability, and sustainability, marking a significant breakthrough in biodiesel production (Magalhães et al., 2020; Turek et al., 2018).

3.6. Physicochemical Properties of Produced Biodiesel and Bio-lubricant

The physicochemical properties of FAME obtained from the co-culture medium under optimal conditions are summarized in Table 9.

Table 9. Physicochemical Properties of the produced FAME

Analysis	Value	Method
Kinematic viscosity (at 40 °C)	**4.8 mm^2/s**	**ASTM D445-17a**
Kinematic viscosity (at 100 °C)	**2.1 mm^2/s**	**ASTM D445-17a**
FAME content	**98.1%**	**Gravimetric analysis**
Iodine number	**101 (g I_2/100 g)**	**ASTM D1959-97**
CFPP	**-3 °C**	**ASTM D6371-17a**
Density (at 15 °C)	**879 kg/m^3**	**ASTM D4052-22**

Pour point	**-1 °C**	**ASTM D97-08**
Acid number	**0.31 (mg KOH/g)**	**ASTM D974-22**
Flash point	**192 °C**	**ASTM D92**
Sulfated ash content	**<0.01 wt.%**	**ASTM D874-23**
Oxidation stability	**8.62 h**	**EN 14112**

The obtained FAME properties align with the EN-14214 standard, confirming its suitability for biodiesel applications. Following the second-stage transesterification using NPG and subsequent blending with performance-enhancing additives, the physicochemical characteristics of the resultant bio-lubricant (NPG triester) were evaluated and are presented in Table 10.

Table 10. Physicochemical Properties of the produced Bio-Lubricant

Analysis	Value	Method
Kinematic viscosity (at 40 °C)	**223 mm^2/s**	**ASTM D445-17a**
Kinematic viscosity (at 100 °C)	**20.2 mm^2/s**	**ASTM D445-17a**
Density (at 15 °C)	**923 kg/m^3**	**ASTM D4052-22**
Pour point	**-11 °C**	**ASTM D97-08**
Acid number	**0.5 (mg KOH/g)**	**ASTM D974-22**
Flash point	**243 °C**	**ASTM D92**
Sulfated ash content	**<0.01 wt.%**	**ASTM D874-23**
Oxidation stability	**>200 h**	**EN 14112**

Analysis of Physicochemical Enhancements in the Bio-Lubricant

A significant increase in kinematic viscosity from 4.8 mm^2/s at 40°C and 2.1 mm^2/s at 100°C for FAME to 223 mm^2/s and 20.2 mm^2/s, respectively, was observed in the bio-lubricant. This enhancement is primarily attributed to the incorporation of PMMA and TiO_2, which strengthened intermolecular forces and increased molecular weight (Abdel Hamid et al., 2024). The density similarly increased from 879 kg/m^3 to 923 kg/m^3, a result of the formation of complex ester structures and enhanced molecular interactions during transesterification with NPG (Crompton et al., 2018).

The pour point showed a notable improvement, decreasing from -1°C in FAME to -11°C in the bio-lubricant, indicating superior low-temperature fluidity. This enhancement is attributed to the branched structure of NPG and the presence of PMMA and BHT, which disrupted crystallization and improved flow properties under cold conditions (Raof et al., 2018).

A slight increase in the acid number, from 0.31 mg KOH/g to 0.5 mg KOH/g, was observed, likely due to minor ester hydrolysis and oxidation side reactions during transesterification (Crompton et al., 2018). Importantly, the flash point improved significantly from 192°C in FAME to 243°C in the NPG triester bio-lubricant. This enhancement is linked to the stabilizing effects of PMMA and TiO_2, which reduced volatility and increased thermal resistance (Silva et al., 2024).

Oxidation stability exceeded 200 hours, a substantial improvement over the 8.62-hour stability of FAME. This remarkable enhancement is primarily due to the presence of BHT, which effectively inhibits free radical propagation and peroxide formation, thereby minimizing oxidative degradation (Li et al., 2022). The incorporation of high-molecular-weight esters and polymeric additives significantly improved the tribological properties, reducing friction and enhancing wear resistance under high-temperature operating conditions.

4. Conclusion and Future Perspectives

The development of NPG triester bio-lubricant through the co-culture of *Rhodosporidium babjevae* and *Arthrospira platensis* in pulp and paper mill sludge represents a significant advancement in sustainable lubrication technology. Comprehensive physicochemical characterization confirmed its superior properties, including high kinematic viscosity (217 mm^2/s at 40°C and 21.2 mm^2/s at 100°C), a reduced pour point (-11°C), an elevated flash point (243°C), and enhanced oxidative stability (>200 hours). These properties closely align with the industrial-grade Shell Gas Compressor Oil S3 PY 220, underscoring its potential applicability in high-temperature and high-load tribological systems, particularly in gas compression applications. The secondary transesterification process, combined with the incorporation of PMMA, BHT, and TiO_2, significantly enhanced its thermal resistance, viscosity stability, and oxidation resistance, making it a robust alternative to conventional petroleum-based lubricants.

Beyond lubrication applications, this research also highlights the dual benefits of biodiesel production and wastewater remediation. The initial transesterification process yielded high-purity FAME with a content of 98.1%, meeting the stringent EN-14214 standards for biodiesel. This biofuel exhibited a kinematic viscosity of 4.8 mm^2/s at 40°C, an iodine number of 101 g I_2/100 g, and excellent oxidation stability (8.62 hours), making it suitable for commercial biodiesel applications. The production of both biodiesel and bio-lubricant from a single microbial system highlights the efficiency of the integrated biorefinery approach.

From a biotechnological standpoint, utilizing the metabolic capabilities of R. babjevae and A. platensis in a controlled co-culture system not only facilitated efficient lipid accumulation (6.683 g/L of extracted lipids), but also contributed to a significant reduction in chemical oxygen demand (COD) (86.762%). This emphasizes the process's dual purpose of creating high-value bio-based goods while also reducing environmental pollutants. Following acid pretreatment, the enzymatic hydrolysis phase was tuned to maximize sugar release, which increased microbial lipid production and improved process sustainability.

Despite its established technological capability, large-scale deployment of this bio-lubricant requires comprehensive tribological testing under real-world operational circumstances, such as extended exposure to intense shear stress, high pressures, and varied temperature cycles. Future study should concentrate on improved rheological modeling, molecular dynamics (MD) simulations, and computational fluid dynamics (CFD) assessments to forecast long-term stability and optimize formulation for industrial-scale deployment. Furthermore, investigating alternate

enzymatic hydrolysis methodologies, innovative co-culture configurations, and metabolic engineering approaches may increase lipid yield while improving the physicochemical qualities of both the biodiesel and bio-lubricant.

To bridge the gap between laboratory-scale production and commercial adoption, the bio-lubricant's compatibility with various industrial systems must be evaluated, notably in the aerospace, automotive, and high-speed rotary machinery sectors. Furthermore, lifecycle assessment (LCA) studies should be carried out to measure its environmental effect in comparison to traditional lubricants and fuels, assuring compliance with circular economy concepts and sustainability objectives. The incorporation of nanomaterials such as graphene-based additives or ionic liquids may also be investigated to improve tribological performance and oxidation resistance.

In conclusion, the development of a bio-lubricant and biodiesel from lignocellulosic waste via microbial co-cultivation presents a viable, eco-friendly alternative to petroleum-based products. With further refinement in process scalability, additive optimization, and in-depth tribological evaluations, this innovation holds significant potential for revolutionizing sustainable energy and lubrication solutions in high-performance engineering applications.

References

Abdel Hamid, E. M., Amer, A. M., Mahmoud, A. K., Mokbl, E. M., Hassan, M. A., Abdel-Monaim, M. O., ... & Tharwat, K. M. (2024). Box-Behnken design (BBD) for optimization and simulation of biolubricant production from biomass using aspen plus with techno-economic analysis. *Scientific Reports*, *14*(1), 21769.

Abu-Ghosh, S., Fixler, D., Dubinsky, Z., & Iluz, D. (2016). Flashing light in microalgae biotechnology. *Bioresource technology*, *203*, 357-363.

Aiba, S., & Ogawa, T. (1977). Assessment of growth yield of a blue—green alga, Spirulina platensis, in axenic and continuous culture. *Microbiology*, *102*(1), 179-182.

Ali, E. N., & Tay, C. I. (2013). Characterization of biodiesel produced from palm oil via base catalyzed transesterification. Procedia Engineering, 53, 7-12.

Alptekin, E., & Canakci, M. (2011). Optimization of transesterification for methyl ester production from chicken fat. *Fuel*, *90*(8), 2630-2638.

An, J., Astapova, I., Zhang, G., Cangelosi, A. L., Ilkayeva, O., Marchuk, H., ... & Newgard, C. B. (2024). Integration of metabolomic and transcriptomic analyses reveals novel regulatory functions of the ChREBP transcription factor in energy metabolism. *bioRxiv*.

Ananthi, V., Raja, R., Carvalho, I. S., Brindhadevi, K., Pugazhendhi, A., & Arun, A. (2021). A realistic scenario on microalgae-based biodiesel production: Third generation biofuel. Fuel, 284, 118965 .

Ariunbaatar, J., Panico, A., Esposito, G., Pirozzi, F., & Lens, P. N. (2014). Pretreatment methods to enhance anaerobic digestion of organic solid waste. *Applied energy*, *123*, 143-156.

Asif, S., Ahmad, M., Zafar, M., & Ali, N. (2017). Prospects and potential of fatty acid methyl esters of some non-edible seed oils for use as biodiesel in Pakistan. *Renewable and Sustainable Energy Reviews*, *74*, 687-702.

Banerjee, C., Dubey, K. K., & Shukla, P. (2016). Metabolic engineering of microalgal based biofuel production: prospects and challenges. *Frontiers in microbiology*, *7*, 432.

Baunillo, K. E., Tan, R. S., Barros, H. R., & Luque, R. (2012). Investigations on microalgal oil production from Arthrospira platensis: towards more sustainable biodiesel production. RSC advances, 2(30), 11267-11272.

Bligh, E. G., & Dyer, W. J. (1959). A rapid method of total lipid extraction and purification. *Canadian journal of biochemistry and physiology*, *37*(8), 911-917. Michelon, M., de Matos de Borba, T., da Silva Rafael, R., Burkert, C. A. V., & de Medeiros Burkert, J. F. (2012). Extraction of carotenoids from Phaffia rhodozyma: A comparison between different techniques of cell disruption. *Food Science and Biotechnology*, *21*, 1-8.

Bouaid, A., Iliuta, G., & Marchetti, J. M. (2024). Cold flow properties of biodiesel from waste cooking oil and a new improvement method. *Heliyon*, *10*(17).

Burlacot, A. (2023). Quantifying the roles of algal photosynthetic electron pathways: a milestone towards photosynthetic robustness. *New Phytologist*, *240*(6), 2197-2203.

Chatterjee, S., & Mohan, S. V. (2018). Microbial lipid production by Cryptococcus curvatus from vegetable waste hydrolysate. Bioresource Technology, 254, 284–289 .

Checa, M., Nogales-Delgado, S., Montes, V., & Encinar, J. M. (2020). Recent advances in glycerol catalytic valorization: A review. *Catalysts*, *10*(11), 1279.

Cheirsilp, B., Suwannarat, W., & Niyomdecha, R. (2011). Mixed culture of oleaginous yeast Rhodotorula glutinis and microalga Chlorella vulgaris for lipid production from industrial wastes and its use as biodiesel feedstock. *New biotechnology*, *28*(4), 362-368.

Cheirsilp, B., Suwannarat, W., & Niyomdecha, R. (2011). Mixed culture of oleaginous yeast Rhodotorula glutinis and microalga Chlorella vulgaris for lipid production from industrial wastes and its use as biodiesel feedstock. New Biotechnology, 28(4), 362–368 .

Chen, L., Lee, J. J. L., Zhang, J., & Chen, W. N. (2016). Comparative proteomic analysis of engineered Saccharomyces cerevisiae with enhanced free fatty acid accumulation. *Applied microbiology and biotechnology*, *100*(3), 1407-1420.

Cheng, Y. T., & Yang, C. F. (2016). Using strain Rhodotorula mucilaginosa to produce carotenoids using food wastes. *Journal of the Taiwan Institute of Chemical Engineers*, *61*, 270-275.

Crompton, M. J., & Dunstan, R. H. (2018). Evaluation of in-situ fatty acid extraction protocols for the analysis of staphylococcal cell membrane associated fatty acids by gas chromatography. *Journal of Chromatography B*, *1084*, 80-88.

Cronan, J. E. (2021). The classical, yet controversial, first enzyme of lipid synthesis: Escherichia coli acetyl-CoA carboxylase. *Microbiology and Molecular Biology Reviews*, *85*(3), 10-1128.

Cui, J., Davanture, M., Zivy, M., Lamade, E., & Tcherkez, G. (2019). Metabolic responses to potassium availability and waterlogging reshape respiration and carbon use efficiency in oil palm. *New Phytologist*, *223*(1), 310-322.

Daels, E., Foubert, I., Guo, Z., Thielemans, W., & Goderis, B. (2020). Phase behavior and polymorphism of saturated and unsaturated phytosterol esters. *Molecules*, *25*(23), 5727.

Encinar, J. M., Nogales-Delgado, S., & Pinilla, A. (2021). Biolubricant production through double transesterification: reactor design for the implementation of a biorefinery based on rapeseed. *Processes*, *9*(7), 1224.

Gao, Y., Guo, L., Liao, Q., Zhang, Z., Zhao, Y., Gao, M., ... & Wang, G. (2021). Mariculture wastewater treatment with Bacterial-Algal Coupling System (BACS): Effect of light intensity on microalgal biomass production and nutrient removal. *Environmental Research*, *201*, 111578.

Ghosh, S., Chowdhury, R., & Bhattacharya, P. (2016). Mixed consortia in bioprocesses: Role of microbial interactions. Applied Microbiology and Biotechnology, 100(10), 4283–4295 .

Godoy, C. A., Valiente, M., Pons, R., & Montalvo, G. (2015). Effect of fatty acids on self-assembly of soybean lecithin systems. *Colloids and Surfaces B: Biointerfaces*, *131*, 21-28.

Goswami, R. K., Agrawal, K., & Verma, P. (2021). Microalgae-based biofuel-integrated biorefinery approach as sustainable feedstock for resolving energy crisis. In Bioenergy research: Commercial opportunities & challenges (pp. 267–293).

Huo, S., Dong, R., Wang, Z., Pang, C., Yuan, Z., Zhu, S., & Chen, L. (2011). Available resources for algal biofuel development in China. *Energies*, *4*(9), 1321-1335.

IEA (International Energy Agency). (2019). Global energy demand rose by 2.3% in 2018, its fastest pace in the last decade. Retrieved from https://www.iea.org

Jackson, M. J., & Line, M. A. (1997). Organic composition of a pulp and paper mill sludge determined by FTIR, 13C CP MAS NMR, and chemical extraction techniques. *Journal of agricultural and food chemistry*, *45*(6), 2354-2358.

Jiang, H., Nie, J., Zeng, L., Zhu, F., Gao, Z., Zhang, A., ... & Chen, Y. (2024). Selective Removal of Hemicellulose by Diluted Sulfuric Acid Assisted by Aluminum Sulfate. *Molecules*, *29*(9), 2027.

Kato, Y., & Hasunuma, T. (2021). Metabolic engineering for carotenoid production using eukaryotic microalgae and prokaryotic cyanobacteria. *Carotenoids: Biosynthetic and Biofunctional Approaches*, 121-135.

Khan, M. I., Shin, J. H., & Kim, J. D. (2018). The promising future of microalgae: Current status, challenges, and optimization of a sustainable and renewable industry for biofuels, feed, and other products. Microbial Cell Factories, 17(1), 36 .

Khoo, C. G., Dasan, Y. K., Lam, M. K., & Lee, K. T. (2019). Algae biorefinery: Review on a broad spectrum of downstream processes and products. Bioresource Technology, 292, 121964 .

Kitcha, S., & Cheirsilp, B. (2014). Enhanced lipid production by co-cultivation and co-encapsulation of oleaginous yeast Trichosporonoides spathulata with microalgae in alginate gel beads. *Applied biochemistry and biotechnology*, *173*, 522-534.

Kulsuwan, N., & Kongkiattikajorn, J. (2012). Study on optimal conditions for reducing sugars production from recycled paper sludge by diluted acid and enzymes. *KKU Res. J.*, *17*, 622-629.

Landolfo, S., Ianiri, G., Camiolo, S., Porceddu, A., Mulas, G., Chessa, R., ... & Mannazzu, I. (2018). CAR gene cluster and transcript levels of carotenogenic genes in Rhodotorula mucilaginosa. *Microbiology*, *164*(1), 78-87.

Lee, Y. R., & Chen, J. J. (2016). Optimization of simultaneous biomass production and nutrient removal by mixotrophic Chlorella sp. using response surface methodology. *Water Science and Technology*, *73*(7), 1520-1531.

Li, S., Tang, S., Li, J., Chen, L., & Ma, Y. (2022). Protective effects of four natural antioxidants on hydroxyl-radical-induced lipid and protein oxidation in Yak Meat. *Foods*, *11*(19), 3062.

Lian, J., Wijffels, R. H., Smidt, H., & Sipkema, D. (2018). The effect of the algal microbiome on industrial production of microalgae. Microbial Biotechnology, 11(5), 806–818 .

Liu, L., Chen, J., Lim, P. E., & Wei, D. (2018). Dual-species cultivation of microalgae and yeast for enhanced biomass and microbial lipid production. Journal of Applied Phycology, 30, 2997–3007 .

Ma, X., Zhang, Y., Song, Z., Yu, K., He, C., & Zhang, X. (2021). Enzyme-catalyzed synthesis and properties of polyol ester biolubricant produced from Rhodotorula glutinis lipid. *Biochemical Engineering Journal*, *173*, 108101.

Magalhães, K. T., de Sousa Tavares, T., & Nunes, C. A. (2020). The chemical, thermal and textural characterization of fractions from Macauba kernel oil. *Food Research International*, *130*, 108925.

Magdouli, S., Brar, S. K., & Blais, J. F. (2016). Co-culture for lipid production: Advances and challenges. Biomass and Bioenergy, 92, 20–30 .

Mathew, M. M., Khatana, K., Vats, V., Dhanker, R., Kumar, R., Dahms, H. U., & Hwang, J. S. (2022). Biological approaches integrating algae and bacteria for the degradation of wastewater contaminants—a review. *Frontiers in Microbiology*, *12*, 801051.

Mathimani, T., & Pugazhendhi, A. (2019). Utilization of algae for biofuel, bio-products and bio-remediation. Biocatalysis and Agricultural Biotechnology, 17, 326–330 .

Matsui, Y., & Iwahashi, H. (2018). Radical formation in individual aqueous solutions of some unsaturated fatty acids and in their mixtures. *Journal of Clinical Biochemistry and Nutrition*, *63*(2), 90-96.

Michelon, M., de Matos de Borba, T., da Silva Rafael, R., Burkert, C. A. V., & de Medeiros Burkert, J. F. (2012). Extraction of carotenoids from Phaffia rhodozyma: A comparison between different techniques of cell disruption. *Food Science and Biotechnology*, *21*, 1-8.

Mohiddin, M. N. B., Tan, Y. H., Seow, Y. X., Kansedo, J., Mubarak, N. M., Abdullah, M. O., ... & Khalid, M. (2021). Evaluation on feedstock, technologies, catalyst and reactor for sustainable biodiesel production: A review. Journal of Industrial and Engineering Chemistry, 98, 60-81.

Moncada, J., & Aristizábal, V. (2016). Design strategies for sustainable biorefineries. *Biochemical Engineering Journal*, *116*, 122-134.

Munch, G., Sestric, R., Sparling, R., Levin, D. B., & Cicek, N. (2015). Lipid production in the under-characterized oleaginous yeasts, Rhodosporidium babjevae and Rhodosporidium diobovatum, from biodiesel-derived waste glycerol. *Bioresource Technology*, *185*, 49-55.

Naicker, J. E., Govinden, R., Lekha, P., & Sithole, B. (2020). Transformation of pulp and paper mill sludge (PPMS) into a glucose-rich hydrolysate using green chemistry: Assessing pretreatment methods for enhanced hydrolysis. *Journal of environmental management*, *270*, 110914.

Nguyen, D. T., Johir, M. A. H., Mahlia, T. I., Silitonga, A. S., Zhang, X., Liu, Q., & Nghiem, L. D. (2024). Microalgae-derived biolubricants: Challenges and opportunities. *Science of the Total Environment*, 176759.

Ottah, V. E., Ezugwu, A. L., Ezike, T. C., & Chilaka, F. C. (2022). Comparative analysis of alkaline-extracted hemicelluloses from Beech, African rose and Agba woods using FTIR and HPLC. *Heliyon*, *8*(6).

Pan-Utai, W., Iamtham, S., Boonbumrung, S., & Mookdasanit, J. (2022). Improvement in the sequential extraction of phycobiliproteins from Arthrospira platensis using green technologies. *Life*, *12*(11), 1896.

Papadaki, A., Fernandes, K. V., Chatzifragkou, A., Aguieiras, E. C. G., Da Silva, J. A. C., Fernandez-Lafuente, R., ... & Freire, D. M. G. (2018). Bioprocess development for biolubricant production using microbial oil derived via fermentation from confectionery industry wastes. *Bioresource technology*, *267*, 311-318.

Patel, A., Karageorgou, D., Rova, E., Katapodis, P., Christakopoulos, P., & Matsakas, L. (2020). An overview of potential oleaginous microorganisms and their role in biodiesel and omega-3 fatty acid-based industries. Microorganisms, 8(3), 434 .

Prabhu, P., Rajan, M. S., Karthick, A., & Venkatesh, R. (2024). Performance evaluation and chemical oxygen demand removal of tannery wastewater through the aerobic–anaerobic route. *Environmental Monitoring and Assessment*, *196*(4), 352.

Pradhan, S., Prasad, L., Madankar, C., & Naik, S. N. (Eds.). (2024). *Lubricants from Renewable Feedstocks*. John Wiley & Sons.

Przygrodzka, E., Binderwala, F., Powers, R., McFee, R. M., Cupp, A. S., Wood, J. R., & Davis, J. S. (2024). Central Role for Glycolysis and Fatty Acids in LH-responsive Progesterone Synthesis. *bioRxiv*, 2024-02.

Qiao, K., Wasylenko, T. M., Zhou, K., Xu, P., & Stephanopoulos, G. (2017). Lipid production in Yarrowia lipolytica is maximized by engineering cytosolic redox metabolism. *Nature biotechnology*, *35*(2), 173-177.

Rabemanolontsoa, H., & Saka, S. (2016). Various pretreatments of lignocellulosics. *Bioresource technology*, *199*, 83-91.

Rana, M. S., Rahim, M. A., Mosharraf, M. P., Tipu, M. F. K., Chowdhury, J. A., Haque, M. R., ... & Chowdhury, A. A. (2023). Morphological, spectroscopic and thermal analysis of cellulose nanocrystals extracted from waste jute fiber by acid hydrolysis. *Polymers*, *15*(6), 1530.

Raof, N. A., Yunus, R., Rashid, U., Azis, N., & Yaakub, Z. (2018). Palm-based neopentyl glycol diester: a potential green insulating oil. *Protein and Peptide Letters*, *25*(2), 171-179.

Ren, T., Zhang, X., Chen, S., Huang, X., & Zhang, X. (2022). Hydrogen peroxide and peroxymonosulfate intensifying Fe− doped NiC− Al2O3− framework− based catalytic ozonation for advanced treatment of landfill leachate: performance and mechanisms. *Science of the Total Environment*, *843*, 156904.

Rodríguez-Chong, A., Ramírez, J. A., Garrote, G., & Vázquez, M. (2004). Hydrolysis of sugar cane bagasse using nitric acid: a kinetic assessment. *Journal of food Engineering*, *61*(2), 143-152.

Roy, C., Sen, P., & Vurimindi, H. (2023). Kinetic modeling and experiments on removal of COD/nutrients from dairy effluent using chlorella and co-culture. *Bioprocess and Biosystems Engineering*, *46*(8), 1099-1110.

Russo, N. P., Ballotta, M., Usai, L., Torre, S., Giordano, M., Fais, G., ... & Concas, A. (2024). Mixotrophic cultivation of Arthrospira platensis (Spirulina) under salt stress: effect on biomass composition, FAME profile and phycocyanin content. Marine Drugs, 22(9), 381.

Sánchez-Solís, A., Lobato-Calleros, O., Moreno-Terrazas, R., Lappe-Oliveras, P., & Neri-Torres, E. (2024). Biodiesel production processes with yeast: A sustainable approach. Energies, 17(2), 302 .

Satoh, S., Ozaki, M., Matsumoto, S., Nabatame, T., Kaku, M., Shudo, T., ... & Chohnan, S. (2020). Enhancement of fatty acid biosynthesis by exogenous acetyl-CoA carboxylase and pantothenate kinase in Escherichia coli. *Biotechnology Letters*, *42*, 2595-2605.

Sforza, E., Pastore, M., Spagni, A., & Bertucco, A. (2018). Microalgae-bacteria gas exchange in wastewater: how mixotrophy may reduce the oxygen supply for bacteria. *Environmental Science and Pollution Research*, *25*, 28004-28014.

Shaker, S., Morowvat, M. H., & Ghasemi, Y. (2021). Bioinformatics analysis and identification of phytoene synthase gene in microalgae. *Recent Patents on Biotechnology*, *15*(3), 216-226.

Sharma, A. K., Sahoo, P. K., Singhal, S., & Joshi, G. (2016). Exploration of upstream and downstream process for microwave assisted sustainable biodiesel production from microalgae Chlorella vulgaris. Bioresource Technology, 216, 793–800 .

Shen, X. F., Xu, Y. P., Tong, X. Q., Huang, Q., Zhang, S., Gong, J., ... & Zeng, R. J. (2022). The mechanism of carbon source utilization by microalgae when co-cultivated with photosynthetic bacteria. *Bioresource Technology*, *365*, 128152.

Shi, F., Wang, Y., Davaritouchaee, M., Yao, Y., & Kang, K. (2020). Directional structure modification of poplar biomass-inspired high efficacy of enzymatic hydrolysis by sequential dilute acid–alkali treatment. *ACS omega*, *5*(38), 24780-24789.

Shtaida, N., Khozin-Goldberg, I., & Boussiba, S. (2015). The role of pyruvate hub enzymes in supplying carbon precursors for fatty acid synthesis in photosynthetic microalgae. *Photosynthesis Research*, *125*, 407-422.

Silva, R. M., Montes-Campos, H., Lobo Ferreira, A. I., Bakis, E., & Santos, L. M. (2024). Thermodynamic study of alkylsilane and alkylsiloxane-based ionic liquids. *The Journal of Physical Chemistry B*, *128*(15), 3742-3754.

Sun, S. N., Chen, X., Tao, Y. H., Cao, X. F., Li, M. F., Wen, J. L., ... & Sun, R. C. (2019). Pretreatment of Eucalyptus urophylla in γ-valerolactone/dilute acid system for removal of non-cellulosic components and acceleration of enzymatic hydrolysis. *Industrial Crops and Products*, *132*, 21-28.

Taherzadeh, M. J., & Karimi, K. (2007). Enzymatic-based hydrolysis processes for ethanol from lignocellulosic materials: A review. *BioResources*, *2*(4), 707-738.

Tahmasebi, Z., Zilouei, H., & Kot, A. M. (2024). Investigating the concomitant production of carotenoids and lipids by the yeast Rhodosporidium babjevae using sugarcane bagasse hydrolysate or corn steep liquor. *Renewable Energy*, *228*, 120618.

Tamaki, S., Mochida, K., & Suzuki, K. (2021). Diverse biosynthetic pathways and protective functions against environmental stress of antioxidants in microalgae. *Plants*, *10*(6), 1250.

Tong, C. Y., Honda, K., & Derek, C. J. C. (2024). Enhancing organic matter productivity in microalgal-bacterial biofilm using novel bio-coating. *Science of The Total Environment*, *906*, 167576.

Turek, K., Domagała, J., & Wszołek, M. (2018). Fatty acid profile and oxidation tests of fat extracted from yogurt using rose hip seed oil. *Acta Scientiarum Polonorum Technologia Alimentaria*, *17*(1), 51-58.

Ugya, A. Y., Chen, H., & Wang, Q. (2024). Microalgae biofilm system as an efficient tool for wastewater remediation and potential bioresources for pharmaceutical product production: an overview. *International Journal of Phytoremediation*, *26*(1), 131-142.

Varela, J. C., Pereira, H., Vila, M., & León, R. (2015). Production of carotenoids by microalgae: achievements and challenges. *Photosynthesis research*, *125*, 423-436.

Veluchamy, C., & Kalamdhad, A. S. (2017). Influence of pretreatment techniques on anaerobic digestion of pulp and paper mill sludge: a review. *Bioresource technology*, *245*, 1206-1219.

Voon, C. P., Law, Y. S., Guan, X., Lim, S. L., Xu, Z., Chu, W. T., ... & Lim, B. L. (2021). Modulating the activities of chloroplasts and mitochondria promotes adenosine triphosphate production and plant growth. *Quantitative Plant Biology*, *2*, e7.

Wahidin, S., Idris, A., & Shaleh, S. R. M. (2013). The influence of light intensity and photoperiod on the growth and lipid content of microalgae Nannochloropsis sp. *Bioresource technology*, *129*, 7-11.

Wang, G., Chen, R., Huang, L., Ma, H., Mu, D., & Zhao, Q. (2018). Microbial characteristics of landfill leachate disposed by aerobic moving bed biofilm reactor. *Water Science and Technology*, *77*(4), 1089-1097.

Wijs, J. J. A. (1929). The Wijs method as the standard for iodine absorption. *Analyst*, *54*(634), 12-14.

Xiao, Y., Guo, J., Zhu, H., Muhammad, A., Deng, H., Hu, Z., & Wu, Q. (2020). Inhibition of glucose assimilation in Auxenochlorella protothecoides by light. *Biotechnology for biofuels*, *13*, 1-13.

Xin, Y., Wu, S., Miao, C., Xu, T., & Lu, Y. (2024). Towards lipid from microalgae: Products, biosynthesis, and genetic engineering. *Life*, *14*(4), 447.

Ye, J., Liang, J., Wang, L., & Markou, G. (2018). The mechanism of enhanced wastewater nitrogen removal by photo-sequencing batch reactors based on comprehensive analysis of system dynamics within a cycle. *Bioresource Technology*, *260*, 256-263.

Yen, H. W., Chen, P. W., & Chen, L. J. (2015). The synergistic effects for the co-cultivation of oleaginous yeast-Rhodotorula glutinis and microalgae-Scenedesmus obliquus on the biomass and total lipids accumulation. Bioresource Technology, 184, 148–152 .

Zhang, L., Lee, J. T., Ok, Y. S., Dai, Y., & Tong, Y. W. (2022). Enhancing microbial lipids yield for biodiesel production by oleaginous yeast Lipomyces starkeyi fermentation: a review. Bioresource technology, 344, 126294.

Zhang, Y., Li, J., Si, L., Gao, M., Wang, S., & Wang, X. (2024). Sudden sulfamethoxazole shock leads to nitrite accumulation in microalgae-nitrifying bacteria consortia: Physiological responses and light regulating strategy. *Journal of Environmental Management*, *366*, 121714.

Zhang, Z., Ji, H., Gong, G., Zhang, X., & Tan, T. (2014). Synergistic effects of oleaginous yeast Rhodotorula glutinis and microalga Chlorella vulgaris for enhancement of biomass and lipid yields. Bioresource Technology, 164, 93–99.